Master's thesis

NTNU
Norwegian University of Science and Technology
Faculty of Information Technology and Electrical Engineering
Department of Electronic Systems

Jenny Aune Forbord

Bayesian range estimate from two-directional phase measurements

Master's thesis in Electronics Systems Design and Innovation
Supervisor: Kimmo Kansanen
Co-supervisor: Carsten Wulff
July 2023

NTNU
Norwegian University of
Science and Technology

Jenny Aune Forbord

Bayesian range estimate from two-directional phase measurements

Master's thesis in Electronics Systems Design and Innovation
Supervisor: Kimmo Kansanen
Co-supervisor: Carsten Wulff
July 2023

Norwegian University of Science and Technology
Faculty of Information Technology and Electrical Engineering
Department of Electronic Systems

NTNU
Norwegian University of
Science and Technology

Abstract

Technology is constantly expanding, and today you can find electronics and software in more and more everyday objects. Being able to determine the position of an object is desirable in many contexts. There are many good positioning solutions for outdoor use, but they are often limited by the environment when entering buildings. Bluetooth Low Energy (BLE) is a radio technology that can be found in many electronic devices. Using already available technology to find an accurate distance between objects will be very convenient.

This master's thesis derives a Bayesian distance estimate for two-directional phase measurements. Here, a two-directional measurement means that a frequency signal is sent both back and forth between two devices, where the phase and amplitude of the signal are measured at both of them. This will be done at multiple frequency channels. The range estimate uses the Signal-to-Noise Ratio (SNR) and phase measurements of both devices for all frequency channels used. The frequency measurements in this thesis are based on BLE radio signals.

In this thesis, it is shown that on simulated signals, the derived distance estimate gives accurate results. The signal-to-noise ratio affects the accuracy. A simulated signal with an SNR of 3 dB resulted in a standard deviation of 6.2 cm on a range estimate of 10.0 meters, while when using a simulated signal with an SNR of 12 dB, there was no deviation.

Sammendrag

Teknologien utvider seg stadig, og i dag kan man finne elektronikk og programvare i mange ulike gjenstander. Å kunne bestemme posisjonen til en gjenstand er i mange sammenhenger ønskelig. Det finnes flere gode posisjonsløsninger for utendørs bruk, men de blir ofte begrenset av omgivelsene inne i bygninger. Bluetooth Low Energy (BLE) er en utbredt radioteknologi som finnes i mange elektroniske enheter. Det å ta i bruk teknologi som allerede er tilgjengelig for å finne avstanden mellom gjenstander vil være veldig praktisk.

Denne masteroppgaven utleder et Bayesiansk avstandsestimat for toveis fasemålinger. Toveis måling vil i denne oppgaven bety at et signal med en gitt frekvens blir sendt frem og tilbake mellom to enheter, hvor fasen og amplituden til signalet blir målt ved begge. Dette blir gjort ved flere frekvenserkanaler. Avstandsestimatet som blir funnet, bruker signal-til-støy-forholdet (SNR) og fasemålinger ved begge enhetene for alle frekvenskanalene. Frekvensmålingene i denne oppgaven baserer seg på radio signalering for BLE.

Det blir vist at på simulerte signaler, vil det utledete avstandsestimatet gi nøyaktige resultater. Nøyaktigheten er avhengig av signal-til-støy-forholdet. Et simulert signal med en SNR på 3 dB resulterte i et standardavvik på 6.2 cm på et avstandsestimat på 10.0 meter, mens for et simulert signal med en SNR på 12 dB var det ikke noe avvik.

Preface

This thesis is written as a part of the five-year master's degree in Electronic System Design and Innovation with specialization in Signal Processing and Communication at the Norwegian University of Science and Technology, NTNU.

I would like to thank my supervisors for their guidance and support. A special thanks to main supervisor Kimmo Kansanen for all discussions and constructive feedback during our weekly meetings.

I would also like to extend my appreciation to my classmates and friends, for giving motivation and for making the years at Gløshaugen fun.

Additionally, I would like to thank my family, especially my parents, for their support and for showing interest in my work.

Table of Contents

List of Figures

Abbreviations

BLE Bluetooth Low Energy

SNR Signal-to-Noise Ratio

IoT Internet-of-Things

RSSI Received Signal Strength Indication

RF Radio Frequency

CT Constant Tone

GPS Global Positioning System

ToA Time-of-Arrival

TDoA Time-Difference-of-Arrival

RT-ToF Round-Trip-Time-of-Flight

MCPD Multi-Carrier Phase-Difference

MAP Maximum a posteriori

PDF Probability Density Function

MMSE Minimum Mean Square Error

LoS Line-of-Sight

Chapter 1

Introduction

1.1 Background and motivation

Outdoors, the location of an object can normally be determined with good accuracy using standard radio-based positioning systems. A well-known example of an accurate outdoor positioning system is Global Positioning System (GPS). Satellite-based positioning do however have limitations when being inside a building. Indoors, environmental factors like walls and roofs can give problems like multipath and signal attenuation [1].

Over the years, an increasing number of everyday objects are connected to the internet and to each other. The network of physical objects with sensors and software being linked together with some wireless connection is often called the Internet-of-Things (IoT). These connected objects share some information. Knowing the distance to, or location of, another object could sometimes be desired. Localization of objects can for example be used for asset tracking, like finding equipment or monitoring items at warehouses, factories, or hospitals. It can also be used for indoor navigation in large buildings, to help users navigate in places like shopping malls, airports, or museums.

Radio localization is a technique where radio signals between a transmitter and a receiver are used to determine where an object is localized. One example of a wireless technology that can use this technique is the popular Bluetooth Low Energy (BLE). For the examples given above, BLE is often used. Besides being a widely used technology, BLE also has very low energy consumption, it is cost-effective, and it is easy to use. Some other typical applications for BLE are music-streaming over speakers, smartwatches, home automation systems, and communications [2].

Using a BLE radio for finding the location indoors is beneficial since it's already utilized in numerous devices, which makes it practical to implement. To find a position, the distance between at least three objects needs to be found. We will now look more into different methods for finding these distances.

1.2 Methods for radio localization

There are different ways to do ranging, the solution will depend on the environment and what kind of signal that is available. The three most used types are those based on the Received Signal

Strength Indication (RSSI), those based on time, and those based on the signal phases.

In the RSSI-based solutions, the attenuation of the Radio Frequency (RF) signal is measured, and the distance is calculated from the decrease of the signal. But since the power of an RF signal can be affected by multipath-fading and interference, these solutions are not very accurate.

Time-based solutions use the propagation delay to calculate the distances. Some commonly used techniques for time-based solutions are Time-of-Arrival (ToA), Time-Difference-of-Arrival (TDoA) and Round-Trip-Time-of-Flight (RT-ToF). A problem with these algorithms is that they need a large bandwidth and strict time synchronization to work well.

In phase-based techniques, the estimation of range will often use the phase shift of the received. The distance estimation in this thesis will be phase-based. More specifically, the thesis will find a range estimate, based on a method called Multi-Carrier Phase-Difference (MCPD), which is based on measurements of the phase difference at multiple frequencies.

1.2.1 The Multi-Carrier Phase-Difference technique for measuring data

The phase-based technique MCPD is compatible with BLE and only needs a coarse synchronization between the sender and receiver clocks. We use a handshake protocol at the two devices we want to know the distance between. The handshake process for one frequency channel is shown in figure 1.1. The initiator will start the process. It sends a Constant Tone (CT), in a given frequency to the reflector. The reflector will then measure the IQ values of this frequency, and send the measurements and the same CT back to the initiator. The initiator will then measure those IQ values before sending a new frequency. The frequency measurements are spread over the whole frequency band for BLE (2.4 GHz - 2.4835 GHz). IQ values are a way to describe the magnitude and the phase of a signal. It gives the in-phase and quadrature measurement, which make it possible to represent a complex signal in two dimensions, and also results in an efficient use of the available bandwidth [3].

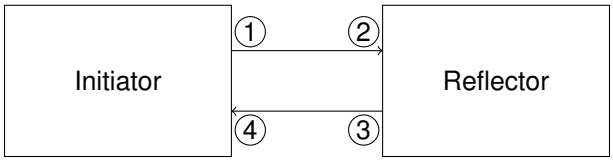

Figure 1.1: Handshake process: The initiator will (1) send a signal, that the reflector (2) will receive and save the values for. The reflector will then (3) send the same signal back to the initiator that will (4) receive and save the values.

Figure 1.2 shows the principle of how the measurement is taken with multiple frequencies. For each frequency channel, the initiator and reflector will both transmit and receive a signal.

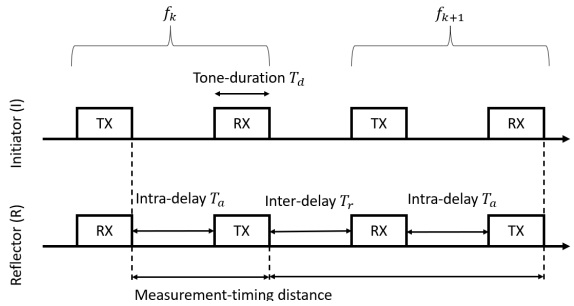

Figure 1.2: The principle of Multi-carrier phase-based ranging.

The details of how the measurements of the MCPD signal are built up, will be described in more detail in section 2.2.

1.3 Goals of the thesis

In this thesis, the focus is to derive an estimation model using the MCPD measuring technique for finding an accurate range estimate for devices using multiple two-directional frequency signals. The estimation will be phase-based.

There are already several solutions out there using the MCPD measuring technique for finding a range estimate. What differs the derivation in this thesis from the others, is the way we look at the measurements. The goal is to examine if it could be beneficial to wait until we find the probability density functions before combining the signals in each direction.

In addition, the estimation model shall be tested with signals at various noise levels, to characterize the performance of the estimate. It shall also be tested over multiple distances, to see if the range will affect the estimate.

Chapter 2

Bayesian range estimation from two-directional phase measurements

In this part of the thesis, the theoretical background to understand the derivation of the estimation model is first presented. The Bayesian philosophy is presented and will be used to estimate the distance. Some ranging methods for the MCPD approach are also described, before there comes some more description about BLE. At the end of the chapter, the signal model and the derivation of a Bayesian range estimate are described.

2.1 Bayesian Estimation

Bayesian estimation is in statistics often used when some prior information about the parameters we are trying to estimate is available. The variables are treated as random, and the prior information is used for finding the posterior distribution [4].

The fundamental of the Bayesian estimation is built on Bayes theorem

$$p(\beta|\mathbf{x}) = \frac{p(\mathbf{x}|\beta)p(\beta)}{p(\mathbf{x})} = \frac{p(\mathbf{x}|\beta)p(\beta)}{\int p(\mathbf{x}|\beta)p(\beta)\,d\beta}, \tag{2.1}$$

where β represents the parameter we want to estimate and **x** represents the observed data. The equation above shows an expression for the posterior Probability Density Function (PDF) for a parameter β, when the observed data **x** is given. The posterior PDF can be found by using the likelihood function $p(\mathbf{x}|\beta)$, which represents the probability of observing the data **x** as a function of the parameters in a statistical model, the prior PDF of the parameter β, $p(\beta)$, and the normalizing constant $p(\mathbf{x})$.

When trying to estimate a parameter, there are often some unknown parameters that are not relevant to the applicable estimate. These are called nuisance parameters, and sometimes they will cause problems when solving an equation. To avoid them, it is possible to integrate them away. Unlike equation (2.1), the signal model sometimes contains multiple parameters that will affect the probability function densities. These can also be integrated away like nuisance parameters. Say that ϵ is the nuisance parameter contained in the posterior PDF, then it can be integrated away

directly from the posterior PDF

$$p(\beta|\mathbf{x}) = \int p(\beta, \epsilon|\mathbf{x})\, d\epsilon. \tag{2.2}$$

2.1.1 Maximum A Posteriori Estimators

When we have calculated the PDF of a variable, there are several ways to find an estimate of the variable. One technique for finding an estimate $\hat{\beta}$ when having the posterior PDF is the Maximum a posteriori (MAP) estimation. It aims to choose the variable β that will maximize, or find the highest mode of the posterior PDF:

$$\hat{\beta} = \arg\max_{\beta}\ p(\beta|\mathbf{x}). \tag{2.3}$$

By using the Bayes rule, we can see that an equivalent maximization would be

$$\hat{\beta} = \arg\max_{\beta}\ \ p(\mathbf{x}|\beta)p(\beta), \tag{2.4}$$

because the normalizing constant $p(\mathbf{x})$ is not dependent on β [4].

2.1.2 Minimum Mean Square Error

Another way to calculate an estimate of a variable in a Bayesian environment is to look at the Minimum Mean Square Error (MMSE). With finite means and variances, the MMSE estimator is given by

$$\tilde{\beta} = E(\beta|\mathbf{x}) = \int \beta\, p(\beta|\mathbf{x})\, d\beta, \tag{2.5}$$

and will be equivalent to at the mean of the posterior PDF. It is the expected value of β given the observations [4].

2.2 The principle of Multi-Carrier Phase-Difference

A good start, when finding a phase measurement, is exploring the shape of the signal. A signal that is not disturbed by any objects from its origin to where it is supposed to be received is called a Line-of-Sight (LoS) signal. The phase shift of a LoS signal can be written as

$$\phi(f, r) = -\frac{2\pi f r}{c_o}, \tag{2.6}$$

where f is the frequency, r is the range, and c_0 is the speed of light in vacuum. The minus sign means that the angle in the model will rotate in a negative direction. The derivation of the phase measurement at the reflector and initiator showed under is based on [5]. For the system explained by figure 1.1 we have two measurements of the phase, one for each direction the signal goes in. At the reflector, the measured phase will be

$$\phi_R(f_k, r) = -2\pi f_k \left(\frac{r}{c_0} - \Delta_t\right) - \theta \pmod{2\pi}, \tag{2.7}$$

with f_k being the k-th frequency, Δ_t being the time offset between the devices and θ being the phase difference for the CT signal between the initiator and reflector. The first term in the equation is the time of flight of the signal, while the two last represents a difference between the offset of the initiator and reflector. When the frequency is sent back, the phase of the signal at the initiator is measured to be

$$\phi_I(f_k, r) = -2\pi f_k \left(\frac{r}{c_0} + \Delta_t \right) + \theta \pmod{2\pi}. \tag{2.8}$$

The difference for these signals is the sign for the time delay and the phase difference.

2.2.1 The ”classical” solutions

Papers like [6] and [5] have after this, added the measured phases from equations (2.7) and (2.8) together. This is to make the phase measurements independent of the time offset and the phase difference between the signals. The difference in phases for one frequency traveling from the initiator to the reflector, and back, will then be

$$\phi_{2W}(f_k, r) = \phi_R(f_k, r) + \phi_I(f_k, r) = -4\pi f_k \frac{r}{c_0} \pmod{2\pi}. \tag{2.9}$$

By looking at the phase difference between neighboring carriers, f_k and f_{k+1}, it is possible to remove the range ambiguity that will come will be

$$\Delta_\phi = \phi_{2W}(f_{k+1}, r) - \phi_{2W}(f_k, r) = -4\pi\Delta_f \frac{r}{c_0} \pmod{2\pi} \tag{2.10}$$

where Δ_f represents the difference between frequencies. An estimate for the range will then be

$$\hat{r} = -\frac{c_0}{4\pi\Delta_f}\hat{\Delta}_\phi \pmod{\frac{c_0}{2\Delta_f}}. \tag{2.11}$$

Notice that the range ambiguity now is $\frac{c_0}{2\Delta_f}$. To get the estimate less sensitive to phase errors, the procedure extends to using K_f frequencies and looking at neighboring phase differences. By taking a sum of the differences, and doing a linear sweep over K_f frequencies, the distance estimate will be given by

$$\hat{r} = -\frac{c_0}{-4\pi\Delta_f(K_f - 1)} \sum_{k=0}^{K_f - 1} \phi_{2W}(f_{k+1}, r) - \phi_{2W}(f_k, r) \tag{2.12}$$

Multiple articles are using this summation of the phases to find an estimate of the range. In [7] and [8] the use of MCPD, IFFT, MUSIC, and slope regression with the summation of the two phases were explored.

2.2.2 The specifications of Bluetooth Low Energy

As mentioned in the introduction, BLE operates in the 2.4 GHz ISM (industrial, Scientific, and Medical) radio frequency band. BLE uses 40 channels in the frequency range from 2.400 GHz to 2.4835 GHz, giving each frequency channel a bandwidth of 2 MHz [9]. With the channel spacing of 2 MHz, the range ambiguity from equation (2.11) will be of 75 meters.

With the 80 MHz band, the frequency is considered to be narrow-band, but with the pseudo-

random frequency hopping of MCPD it could be considered as a wide-band signal. In our signal model, we will use the same base frequency band, but with 80 carrier frequencies. This means we have a carrier spacing of 1 MHz. With a frequency spacing now at 1 MHz, the range ambiguity from equation (2.11) will be of 150 meters. BLE can have a range of up to 100 meters, so this range ambiguity fits the ranging on BLE signals [10].

2.3 Derivation of the signal model

In this thesis, the goal is to look into if there are other ways to find a range estimate, than just to sum the phases from equation (2.7) and (2.8) together. Here we will try to derive an expression for a signal model using a two-directional range estimation technique, using multiple frequency measurements.

The signal model for the signal sent from the initiator to the reflector is given by

$$y_1[f] = A_1[f] \cdot e^{j(-\frac{2\pi f r}{c_0} + \Delta\phi[f])} + w_1[f], \tag{2.13}$$

where $A_1[f]$ is the amplitude for the given frequency f, $\Delta\phi$ is the phase offset in the devices and $w_1[f]$ is the noise, which is expected to be Gaussian distributed with zero mean and variance σ^2. By comparing the phase of this equation with the phase equations given by (2.7) and (2.8), the phase offset and the time offset will have the relationship $\Delta\phi = 2\pi f \Delta_t - \theta$ and will be the same for both the initiator and the reflector. The signal model for the signal sent from the reflector to the initiator is given by

$$y_2[f] = A_2[f] \cdot e^{j(-\frac{2\pi f r}{c_0} - \Delta\phi[f])} + w_2[f], \tag{2.14}$$

where $A_2[f]$ is the amplitude for the given frequency, and $w_2[f]$ is the noise, which also is expected to be Gaussian distributed with zero mean and variance σ^2.

For the measured data we expect the data for the initiator to the reflector to look like

$$y_1'[f] = B_1[f] \cdot e^{-j\theta_1[f]}, \tag{2.15}$$

where $B_1[f]$ is the measured amplitude at the reflector for the given frequency, and $\theta_1[f]$ is the phase measured at the reflector. The signal from the reflector to the initiator can be represented as

$$y_2'[f] = B_2[f] \cdot e^{-j\theta_2[f]}, \tag{2.16}$$

where $B_2[f]$ is the measured amplitude at the initiator for the given frequency, and $\theta_2[f]$ is the phase measured at the initiator.

The phase offset is as explained above, a parameter that will change constantly for each frequency over a time offset in the devices. It will be uniformly distributed between 0 and 2π and has a probability distribution given by $p(\Delta\phi) = \frac{1}{2\pi}$. Since we have assumed that the noise follows a Gaussian distribution, we can also assume that the distribution of the likelihood function follows a Gaussian distribution. This implies that for the observations **x** given the mean μ and variance σ^2, the likelihood function can be written as

$$p(\mathbf{x}|\mu, \sigma^2) = \frac{1}{\sqrt{2\pi\sigma^2}} e^{-\frac{(\mathbf{x}-\mu)^2}{2\sigma^2}}. \tag{2.17}$$

When using MAP to find the distance estimate, we are looking for the parameter that gives the highest posterior probability. By starting to look at one or two frequencies, it is easy to expand when an expression first is found. Our goal is to eventually find a closed form expression for the estimator. So we first work our way to find the range estimate for two frequencies, which is given by

$$\begin{aligned}\hat{r} &= \arg\max_r \, p(r|y_1[f_1], y_2[f_1], y_1[f_2], y_2[f_2]) \\ &= \arg\max_r \, p(r|y_1[f_1], y_2[f_1])\, p(r|y_1[f_2], y_2[f_2]),\end{aligned} \tag{2.18}$$

where y_1 and y_2 are the measurements in each direction, and f_1 and f_2 are the two different frequencies. We can separate the posterior PDFs since the noises of the signals are all independent and identically distributed for each of the frequencies.

To be able to find the final expression, some relevant models are first described. A more thoroughly derivation of these models is found in appendix A. As seen from equation (2.18), the signal model is built up by the posterior PDF of each frequency. This means we can find an expression at one frequency first, and then expand to two and multiple frequencies.

We start by looking at a simplified model for a one-directional signal with noise, then a phase offset is added to the signal model, before we look at the model when the signal is two-directional. In the simple models, we try to determine the probability distributions for the phase ϕ_d instead of the range r, because they make the expression easier. The phase ϕ_d and the range r are connected, as shown in equation (2.6). In the simple models we only look at one frequency, and therefore not directly mention the frequency used. As pointed out in the theory section, the derivation of the different signal models shown here will be treated as a Bayesian estimation problem.

2.3.1 One-directional signal with noise

One of the simplest models to look at is a one-directional signal with noise. The signal y is given by

$$y = A \cdot e^{j\phi_d} + w, \tag{2.19}$$

where A is the amplitude of the given frequency, ϕ_d is the phase at the given frequency, and w is noise for the measured signal. The phase ϕ_d is uniformly distributed between 0 and 2π and has a probability distribution given by $p(\phi_d) = \frac{1}{2\pi}$. When measuring, the signal will have the shape $y' = B \cdot e^{j\theta}$, where B is the measured amplitude and θ is the measured phase.

A posterior PDF must be determined to find a suitable estimator.

The posterior PDF of the phase is dependent on the signal and can be found by looking at the prior information we have of the measured signal and the characteristics given the phase, which is given by

$$p(\phi_d|y) = \frac{p(y|\phi_d)p(\phi_d)}{\int_0^{2\pi} p(y|\phi_d)p(\phi_d)d\phi_d}. \tag{2.20}$$

The likelihood function tells us how the signal y is distributed when we know the characteristics of the phase ϕ_d, and it is given by

$$p(y|\phi_d) = \frac{1}{\sqrt{2\pi\sigma^2}} \cdot \exp\left\{\frac{-|y'|^2 - |A|^2 + 2AB\cos(\phi_d + \theta)}{2\sigma^2}\right\}. \tag{2.21}$$

Setting this and the prior PDF into the expression for the posterior PDF, after some scaling we get a posterior PDF given by

$$p(\phi_d|y) = \frac{\exp\left\{\frac{AB\cos(\phi_d+\theta)}{\sigma^2}\right\}}{2\pi I_0\left(\frac{AB}{\sigma^2}\right)}, \tag{2.22}$$

where $I_0(\cdot)$ represents the modified Bessel function [11]. By using MAP estimation, the phase estimate will be given by

$$\begin{aligned}\hat{\phi_d} &= \arg\max_{\phi_d} p(\phi_d|y) \\ &= -\theta + n \cdot 2\pi,\end{aligned} \tag{2.23}$$

where n is an integer. This shows that when there is no noise or phase offset, the estimator for the phase is given by the measured phase. The estimate has phase ambiguity, so it could have multiple values, but they correspond to the same angle. Given the starting point for this signal, this is a reasonable estimator. For the signal, we were only expecting some white Gaussian noise with zero mean. When calculating an estimator, we can expect the PDF that is biggest to be the one that is closest to the true parameter. The estimation of the phase has a negative sign of the measured phase. From equation (2.6), the sign is also set to be negative, this means we have a negative rotation of the phase.

2.3.2 One-directional signal with noise and phase offset

As explained earlier in this chapter, the phase offset is something that will be in the devices, and it will affect the measurements. Now, we are looking at a one-directional signal with both a phase offset $\Delta\phi$ and noise w. The signal model is now given by

$$y = A \cdot e^{j(\phi_d+\Delta\phi)} + w. \tag{2.24}$$

The signal we will be measuring will have the form $y' = B \cdot e^{j(-\theta+\Delta\phi)}$. The phase offset is not relevant in our estimations and will be treated as a nuisance parameter that we will try to remove. For the posterior PDF, this means we have an equation given by

$$p(\phi_d|y) = \int_0^{2\pi} p(\phi_d, \Delta\phi|y)\, d\Delta\phi. \tag{2.25}$$

Both ϕ_d and $\Delta\phi$ are uniformly distributed between 0 and 2π, which means their posterior PDF is given by

$$p(\phi_d, \Delta\phi|y) = \frac{p(y|\phi_d, \Delta\phi)p(\phi_d, \Delta\phi)}{\int_0^{2\pi}\int_0^{2\pi} p(y|\phi_d, \Delta\phi)p(\phi_d, \Delta\phi)\, d\phi_d\, d\Delta\phi}. \tag{2.26}$$

The prior PDF of ϕ_d and $\Delta\phi$ will be independent of each other and given by $p(\phi_d, \Delta\phi) = p(\phi_d)\, p(\Delta\phi) = \frac{1}{4\pi^2}$. The likelihood function for y will then be

$$p(y|\phi_d, \Delta\phi) = \frac{1}{\sqrt{2\pi\sigma^2}} \cdot \exp\left\{\frac{-|y'|^2 - |A|^2 + 2AB\cos(\phi_d + 2\Delta\phi - \theta)}{2\sigma^2}\right\}. \tag{2.27}$$

The posterior PDF that still contains the nuisance parameter will then be

$$
\begin{aligned}
p(\phi_d, \Delta\phi|y) &= \frac{p(y|\phi_d, \Delta\phi)p(\phi_d, \Delta\phi)}{\int_0^{2\pi}\int_0^{2\pi} p(y|\phi_d, \Delta\phi)p(\phi_d, \Delta\phi)\, d\phi_d\, d\Delta\phi} \\
&= \frac{\exp\left\{\frac{AB\cos(\phi_d+2\Delta\phi-\theta)}{\sigma^2}\right\}}{4\pi^2 \cdot I_0\left(\frac{AB}{\sigma^2}\right)}.
\end{aligned} \tag{2.28}
$$

With values for the amplitude and standard deviation, the denominator of the expression will become a constant. Removing the nuisance parameter $\Delta\phi$ from the expression, the posterior PDF will be given by

$$
p(\phi_d|y) = \int_0^{2\pi} p(\phi_d, \Delta\phi|y)\, d\Delta\phi = \frac{1}{2\pi}, \tag{2.29}
$$

which shows that a posteriori distribution of the phase is uniformly distributed. However, this tells us that we don't have any information about the actual phase. We only have one phase observation and the phase of our signal will have an unknown phase offset, which makes it impossible to find the phase with only this one measurement. That is why we now will expand the signal model to go in two directions. It is expected that the phase offset is constant in both directions.

2.3.3 Two-directional signal with noise and phase offset

From here and out, the estimation will be done for the range r instead of the phase ϕ_d. As mentioned earlier, they are connected with the relationship shown in equation (2.6). From this, it is possible to find that the probability for the range r is also uniformly distributed and given by $p(r) = \frac{2f}{c_0}$. From here an estimate of what the signal could look like will start to emerge. Therefore the signal in this section is written for a specific frequency f. We are still looking at a two-direction frequency signal and have now added noise and phase offset to the model. Our signal is now given as presented in (2.13) and (2.14), with y_1 given by

$$
y_1[f] = A_1[f] \cdot e^{j(-\frac{2\pi f r}{c_0} + \Delta\phi[f])} + w_1[f]
$$

and y_2 given by

$$
y_2[f] = A_2[f] \cdot e^{j(-\frac{2\pi f r}{c_0} - \Delta\phi[f])} + w_2[f].
$$

The signals will both be dependent on the range, but independent of each other. This gives the joint PDF as

$$
p(y_1[f], y_2[f]|r, \Delta\phi[f]) = p(y_1[f]|r, \Delta\phi[f]) \cdot p(y_2[f]|r, \Delta\phi[f]). \tag{2.30}
$$

The PDF of the signals y_1 and y_2 are similar, but not equal. Here y_1 represents the signal from the initiator to the reflector, while y_2 represents the signal from the reflector to the initiator. The PDF of signal y_1 is given by

$$
\begin{aligned}
&p(y_1[f]|r, \Delta\phi[f]) \\
&= \frac{1}{\sqrt{2\pi\sigma^2}} \exp\left\{\frac{\text{-}|y_1'[f]|^2\text{-}|A_1[f]|^2 + 2A_1[f]B_1[f]\cos(\frac{\text{-}2\pi f r}{c_0} + \Delta\phi[f] - \theta_1[f])}{2\sigma^2}\right\},
\end{aligned} \tag{2.31}
$$

where $y_1'[f] = B_1[f] \cdot e^{j\theta_1[f]}$ is the observed signal in coordinates.

For the signal y_2, the PDF is given by

$$\begin{aligned} &p(y_2[f]|r, \Delta\phi[f]) \\ &= \frac{1}{\sqrt{2\pi\sigma^2}} \exp\left\{ \frac{-|y_2'[f]|^2 - |A_2[f]|^2 + 2A_2[f]B_2[f]\cos(\frac{-2\pi fr}{c_0} - \Delta\phi[f] - \theta_2[f])}{2\sigma^2} \right\}, \end{aligned} \tag{2.32}$$

where $y_2'[f] = B_2[f] \cdot e^{j\theta_2[f]}$ is the observed signal at the initiator.

The joint PDF will then become

$$\begin{aligned} &p(y_1[f], y_2[f]|r, \Delta\phi[f]) = p(y_1[f]|r, \Delta\phi[f]) \cdot p(y_2[f]|r, \Delta\phi[f]) \\ &= \frac{1}{2\pi\sigma^2} \exp\left\{ \frac{-|y_1'[f]|^2 - |y_2'[f]|^2 - |A_1[f]|^2 - |A_2[f]|^2}{2\sigma^2} \right\} \\ &\cdot \exp\left\{ \frac{2A_1[f]B_2[f]\cos(-\frac{2\pi fr}{c_0} + \Delta\phi - \theta_1[f]) + 2A_2[f]B_1[f]\cos(-\frac{2\pi fr}{c_0} - \Delta\phi[f] - \theta_2[f])}{\sigma^2} \right\}. \end{aligned} \tag{2.33}$$

We are focusing on the phases, and not the amplitudes. We are assuming we know the amplitudes perfectly, such that $A_1 = B_1$ and $A_2 = B_2$. The signal is also assumed to be equally significant when being measured at the reflector, as when it is being measured at the initiator. Due to their nearly identical travel distances and durations, we denote $A_1 = A_2 = A$ henceforth. It is worth emphasizing that the measurements will not yield perfect equality due to inherent measurement noise. However, this assumption simplifies the derivation process, as the precise estimation of amplitudes is not the primary objective. The joint PDF will therefore be given by

$$\begin{aligned} &p(y_1[f], y_2[f]|r, \Delta\phi[f]) \\ &= \frac{1}{2\pi\sigma^2} \exp\left\{ \frac{-|y_1'[f]|^2 - |y_2'[f]|^2 - 2|A[f]|^2}{2\sigma^2} \right\} \\ &\cdot \exp\left\{ \frac{A[f]^2 \left(\cos(-\frac{2\pi fr}{c_0} + \Delta\phi - \theta_1[f]) + \cos(\frac{2\pi fr}{c_0} - \Delta\phi[f] - \theta_2[f]) \right)}{\sigma^2} \right\} \\ &= \frac{1}{2\pi\sigma^2} \exp\left\{ \frac{-|y_1'[f]|^2 - |y_2'[f]|^2 - 2|A[f]|^2}{2\sigma^2} \right\} \\ &\cdot \exp\left\{ \frac{2A[f]^2 \left(\cos(\frac{2\pi fr}{c_0} + \frac{\theta_1[f]+\theta_2[f]}{2}) \cos(\Delta\phi[f] - \frac{\theta_1[f]-\theta_2[f]}{2}) \right)}{\sigma^2} \right\}. \end{aligned} \tag{2.34}$$

The a-priori probability of both r and $\Delta\phi$ is constant and not dependent on each other. This gives the probability of both of them to be $p(r, \Delta\phi) = \frac{f}{\pi c_0}$. By adding these to the posterior distribution for r and $\Delta\phi$, we get that the prior PDF is given by

$$\begin{aligned} p(r, \Delta\phi[f]|y_1[f], y_2[f]) &= \frac{p(y_1[f], y_2[f]|r, \Delta\phi[f])p(r, \Delta\phi[f])}{\int_0^{2\pi} \int_0^{-\frac{-c_0}{f}} p(y_1[f], y_2[f]|r, \Delta\phi[f])p(r, \Delta\phi[f])\, dr\, d\Delta\phi} \\ &= \frac{\exp\left\{ \frac{2A[f]^2 \left(\cos(\frac{2\pi fr}{c_0} + \frac{\theta_1[f]+\theta_2[f]}{2}) \cos(\Delta\phi[f] - \frac{\theta_1[f]-\theta_2[f]}{2}) \right)}{\sigma^2} \right\}}{K_n[f]}. \end{aligned} \tag{2.35}$$

Where K_n is a normalizing factor that will not affect the extreme points when trying to find the

distance r, but is given by

$$K_n = \int_0^{2\pi} \int_0^{-\frac{c_0}{f}} \cdot \exp\left\{ \frac{2A[f]^2 \left(\cos(\frac{2\pi f r}{c_0} + \frac{\theta_1[f]+\theta_2[f]}{2}) \cos(\Delta\phi[f] - \frac{\theta_1[f]-\theta_2[f]}{2}) \right)}{\sigma^2} \right\} dr\, d\Delta\phi. \quad (2.36)$$

By double integrating, this parameter will not depend on r. The next step is to remove the phase offset $\Delta\phi$, because this is a nuisance parameter. The nuisance parameter can be integrated away, giving us an expression for the posterior PDF of the range:

$$\begin{aligned} p(r|y_1[f], y_2[f]) &= \int_0^{2\pi} p(r, \Delta\phi|y_1[f], y_2[f])\, d\Delta\phi \\ &= \frac{2\pi}{K_n[f]} \cdot I_0 \left(2\frac{A[f]^2}{\sigma^2} \cdot \cos(\frac{2\pi f r}{c_0} + \frac{\theta_1[f]+\theta_2[f]}{2}) \right). \end{aligned} \quad (2.37)$$

To find an estimate of r, the maximum a posteriori (MAP) probability estimation can be used. This involves finding the argument r that maximizes the posterior probability that we found above:

$$\begin{aligned} \hat{r}[f] &= \arg\max_r\, p(r|y_1[f], y_2[f]) \\ &= \arg\max_r\, \frac{2\pi}{K_n[f]} \cdot I_0 \left(\frac{2A[f]^2}{\sigma^2} \cdot \cos\left(\frac{2\pi f r}{c_0} + \frac{\theta_1[f]+\theta_2[f]}{2} \right) \right). \end{aligned} \quad (2.38)$$

The equation above is maximized when the inside of the brackets to the cosine equals zero. This gives us that the MAP estimate of r is given by

$$\hat{r}[f] = -\frac{c_0}{4\pi} \frac{\theta_1[f] + \theta_2[f]}{f}, \quad (2.39)$$

where θ_1 and θ_2 represent the signal's angle of arrival at the reflector and initiator, respectively.

2.3.4 With multiple frequencies

Now have derived the parts needed to find the expression for the estimate in equation (2.18). We will here expand the estimation of what we found to apply to multiple frequencies. We will first look at two, and then expand to multiple frequency channels.

The joint probability for two frequencies in the signal model described over will be given by

$$
\begin{aligned}
p(r|y_1[f_1], y_2[f_1], y_1[f_2], y_2[f_2]) &= \int_0^{2\pi}\int_0^{2\pi} p(r, \Delta\phi_1, \Delta\phi_2|y_1[f_1], y_2[f_1], y_1[f_2], y_2[f_2])\, d\Delta\phi_1\, d\Delta\phi_2 \\
&= \int_0^{2\pi}\int_0^{2\pi} p(r, \Delta\phi_1, \Delta\phi_2|y_1[f_1], y_2[f_1]) \cdot p(r, \Delta\phi_1, \Delta\phi_2|y_1[f_2], y_2[f_2])\, d\Delta\phi_1\, d\Delta\phi_2 \\
&= \int_0^{2\pi}\int_0^{2\pi} p(r, \Delta\phi_1|y_1[f_1], y_2[f_1]) \cdot p(r, \Delta\phi_2|y_1[f_2], y_2[f_2])\, d\Delta\phi_1\, d\Delta\phi_2 \\
&= \int_0^{2\pi} p(r, \Delta\phi_1|y_1[f_1], y_2[f_1])\, d\Delta\phi_1 \cdot \int_0^{2\pi} p(r, \Delta\phi_2|y_1[f_2], y_2[f_2])\, d\Delta\phi_2 \\
&= p(r|y_1[f_1], y_2[f_1]) \cdot p(r|y_1[f_2], y_2[f_2]).
\end{aligned}
\tag{2.40}
$$

The second equation comes from the fact that the two measurements for different frequencies are independent of each other. The third equation above can be shown to be correct, because $y_1[f_1]$ and $y_2[f_1]$ are not dependent on $\Delta\phi_2$, while $y_1[f_2]$ and $y_2[f_2]$ are not dependent on $\Delta\phi_1$.

Here it is possible to insert the equation found in (2.37), for each of the frequencies. The equation for the posterior is now given by

$$
\begin{aligned}
&p(r|y_1[f_1], y_2[f_1], y_1[f_2], y_2[f_2]) \\
=&\frac{2\pi}{K_n[f_1]} \cdot I_0\left(2\frac{A[f_1]^2}{\sigma^2} \cdot \cos\left(\frac{2\pi f_1 r}{c_0} + \frac{\theta_1[f_1] + \theta_2[f_1]}{2}\right)\right) \\
&\cdot \frac{2\pi}{K_n[f_2]} \cdot I_0\left(2\frac{A[f_2]^2}{\sigma^2} \cdot \cos\left(\frac{2\pi f_2 r}{c_0} + \frac{\theta_1[f_2] + \theta_2[f_2]}{2}\right)\right).
\end{aligned}
\tag{2.41}
$$

MAP can also here be used to find the estimate of the distance. MAP for this function is found by:

$$
\begin{aligned}
\hat{r} &= \arg\max_r\ p(r|y_1[f_1], y_2[f_1], y_1[f_2], y_2[f_2]) \\
&= \arg\max_r\ \frac{2\pi}{K_n[f_1]} \cdot I_0\left(2\frac{A[f_1]^2}{\sigma^2} \cdot \cos\left(\frac{2\pi f_1 r}{c_0} + \frac{\theta_1[f_1] + \theta_2[f_1]}{2}\right)\right) \\
&\quad \cdot \frac{2\pi}{K_n[f_2]} \cdot I_0\left(2\frac{A[f_2]^2}{\sigma^2} \cdot \cos\left(\frac{2\pi f_2 r}{c_0} + \frac{\theta_1[f_2] + \theta_2[f_2]}{2}\right)\right) \\
&= \arg\max_r \left(\log\left(I_0\left(\frac{2A[f_1]^2}{\sigma^2} \cdot \cos\left(\frac{2\pi f_1 r}{c_0} + \frac{\theta_1[f_1] + \theta_2[f_1]}{2}\right)\right)\right)\right. \\
&\quad \left. + \log\left(I_0\left(\frac{2A[f_2]^2}{\sigma^2} \cdot \cos\left(\frac{2\pi f_2 r}{c_0} + \frac{\theta_1[f_2] + \theta_2[f_2]}{2}\right)\right)\right)\right).
\end{aligned}
\tag{2.42}
$$

The multiplying factor $\frac{2\pi}{K_{n_i}}$ can be neglected since it is not dependent on the range r. The expression can be rewritten to be a sum of the two frequencies

$$
\hat{r} = \arg\max_r \sum_{i=1}^{2} \log\left(I_0\left(\frac{2A[f_i]^2}{\sigma^2} \cdot \cos\left(\frac{2\pi f_i r}{c_0} + \frac{\theta_1[f_i] + \theta_2[f_i]}{2}\right)\right)\right). \tag{2.43}
$$

Subsequently, this can be expanded for multiple frequencies. The expression of the range estim-

ate can for K_f frequencies be expanded to

$$\hat{r} = \arg\max_r \sum_{i=1}^{K_f} \log\left(I_0\left(\frac{2A[f_i]^2}{\sigma^2} \cdot \cos\left(\frac{2\pi f_i r}{c_0} + \frac{\theta_1[f_i] + \theta_2[f_i]}{2}\right)\right)\right). \tag{2.44}$$

The modified Bessel function $I_0(\cdot)$ is by itself exponentially growing, and will therefore, in this expression, be maximized when the cosine is 1. The cosine is 1 when the argument is zero or equal to some integer multiple of 2π, $\frac{2\pi f_i r}{c_0} + \frac{\theta_1[f_i]+\theta_2[f_i]}{2} = n \cdot 2\pi$, where n is an integer. In other words, the function will have a maximum where the average phase of the measured phases θ_1 and θ_2 is the same as the calculated phase for the correct range estimate.

It is also worth noticing that the estimator will for each frequency have a different Signal-to-Noise Ratio (SNR), here given by $\frac{A[f_i]^2}{\sigma^2}$. This means that the model therefore should be able to adjust for measurements that have non-constant SNR over the different frequencies.

We now have an expression for a range estimate with K_f frequency channels and will test how good this estimator is.

2.4 Using MMSE for one frequency

We have also tried to find an MMSE estimator. An attempt was first made to find a solution with one frequency. Equation (2.5) shows that to find an estimate using MMSE, we need to integrate the posterior PDF with the variable we want to estimate.

By setting in our variables, we get that the MMSE can be written as

$$\tilde{r} = E(r|\mathbf{y}) = \int_0^{\frac{c_0}{f}} r \cdot p(r|\mathbf{y})\, dr. \tag{2.45}$$

Using the posterior PDF found in equation (2.37), we find that the MMSE estimator will be given by

$$\tilde{r} = \int_0^{\frac{c_0}{f}} r \cdot \frac{2\pi}{K_n[f]} \cdot I_0\left(\frac{2A[f]^2}{\sigma^2} \cdot \cos\left(\frac{2\pi f r}{c_0} + \frac{\theta_1[f] + \theta_2[f]}{2}\right)\right) dr. \tag{2.46}$$

After a thorough review, the conclusion is that this expression will result in a non-trivial solution, and will therefore not be followed further. The review can be found in Appendix B.

Chapter 3

Results

To determine if the expression we have found in equation (2.44) works for range estimation, we need to test it. The following tests have been conducted using simulated data:

- for one distance, with multiple frequencies and high SNR.
- for one distance, with multiple frequencies over multiple SNR.
- for multiple distances, with multiple frequencies and a set SNR

The first test is used to visualize the characteristics of the posterior PDF. From this, we can see more clearly how the model is working, and better observe how we can use the characteristics to determine the distance.

The second test is to investigate how the performance of the model changes with different noise levels added to the signal. This is used to characterize the performance of the estimator at different noise levels.

The third test is used to check if the distance between the devices will affect the range estimate. It is therefore tested at distances in the range of BLE, from 0 to 100 meters. We have in this test used a signal with the same signal strength at all distances to characterize the estimator error as a function of range. Even though a real-world signal will attenuate with distance, we will not consider that in this test.

The code for the estimation of the simulated data is found in appendix D.

3.1 Characteristics of the simulated data

In the first test, there is simulated a signal with an SNR of 10 dB. Before the noise is added, the angle of the signal is defined from equation (2.6), with the range being a set distance and the frequency bands are the 80 frequencies from the BLE frequency band.

We are testing if the estimation model found in equation (2.44) is a good estimator for finding the range when looking at multiple frequencies. The model aims to find the distance that has the highest posterior PDF. It is run with a brute-force approach, checking multiple distances to see which one is more likely. Figure 3.1 shows how the probability densities are for distances

between 5 and 15 meters when having the grid set to check every 1.7 cm and the true distance of the simulation set to be 10.0 meters.

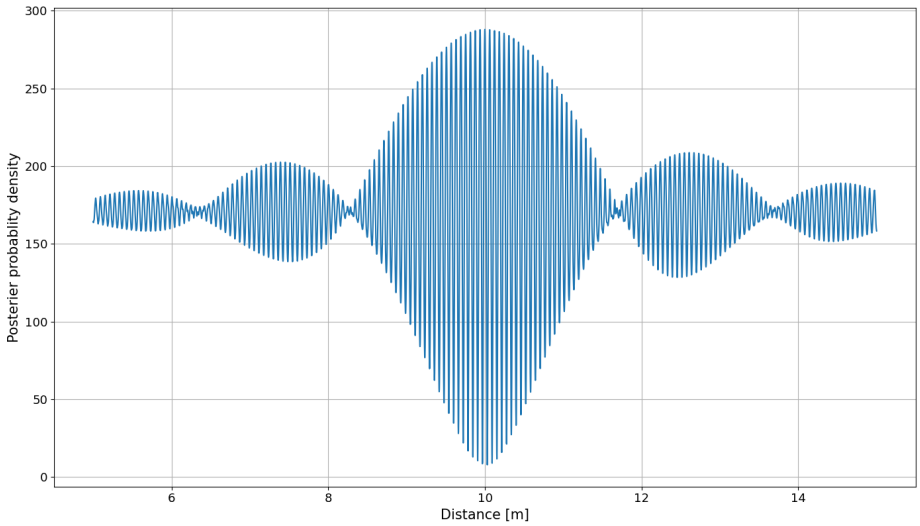

Figure 3.1: Posterior PDF for simulated data for 10 meters.

The distance with the highest probability is 10.0 meters. This corresponds to the distance set in the signal model. From the figure, it is possible to see that the signal is in the y-axis spread around a value of 170. In the x-axis, the main lobe is concentrated around 10 meters.

The envelope of the posterior PDF has the shape of a sinc function. The shape of the distribution comes from the phases inside the cosine in the expression for the estimate in (2.44). It will be dependent on both the range and the frequency. Zooming in on the main lobe of the envelope, the characteristics of the signal are highlighted. A zoomed-in version of the main lobe is shown in figure 3.2, showing that the form of the main lobe is made from smaller sine-like waves.

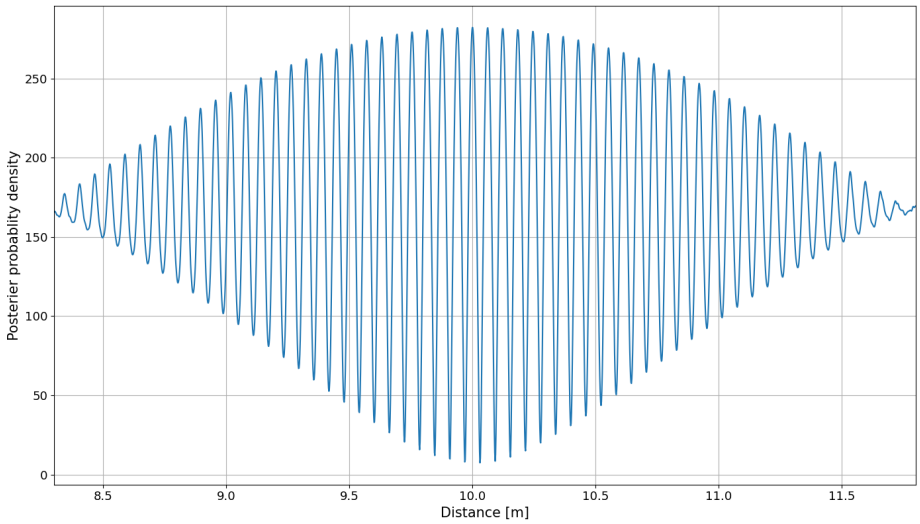

Figure 3.2: The main lobe of the posterior PDF.

Figure 3.3 shows the three sine curves with the highest amplitude. The second largest wave gives a distance of 9.938 meters, giving a distance to the top of 6.2 cm. Using equation (2.6) and the fact that the phase is 2π periodic, we have that the wavelength of the signal is $\lambda = 12.5$ cm. This shows that the posterior PDF is periodic with a half wavelength of the signal.

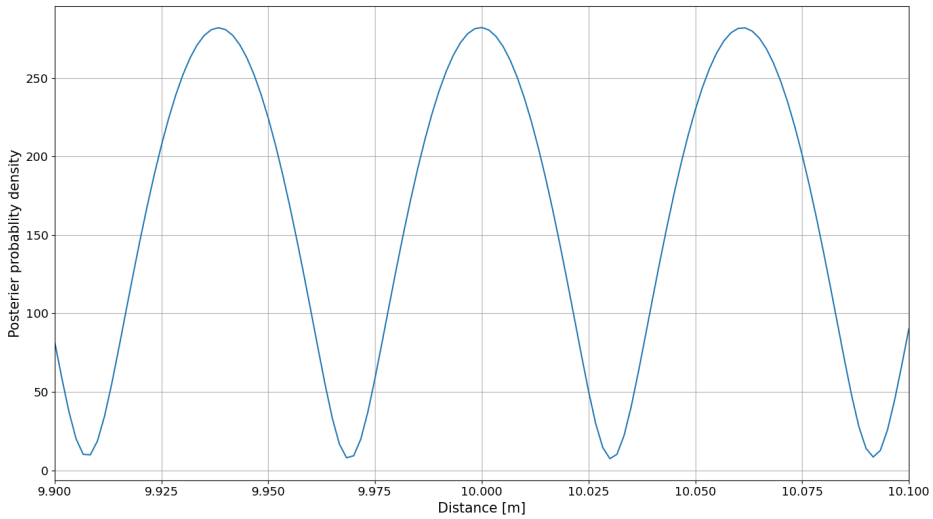

Figure 3.3: The three middle waves in the main lobe.

By increasing the noise in the signal so that the signal has a SNR of 0 dB for the same set distance, the probability distributions when testing for multiple distances are shown in figure 3.4. Here the distance with the highest probability is 9.97 meters.

This shows that even for high noise, this range estimate can be used, but the accuracy will be decreased. From the posterior PDF-plot, it can be seen when zoomed in, that it looks like the highest waves in the signal are slightly shifted.

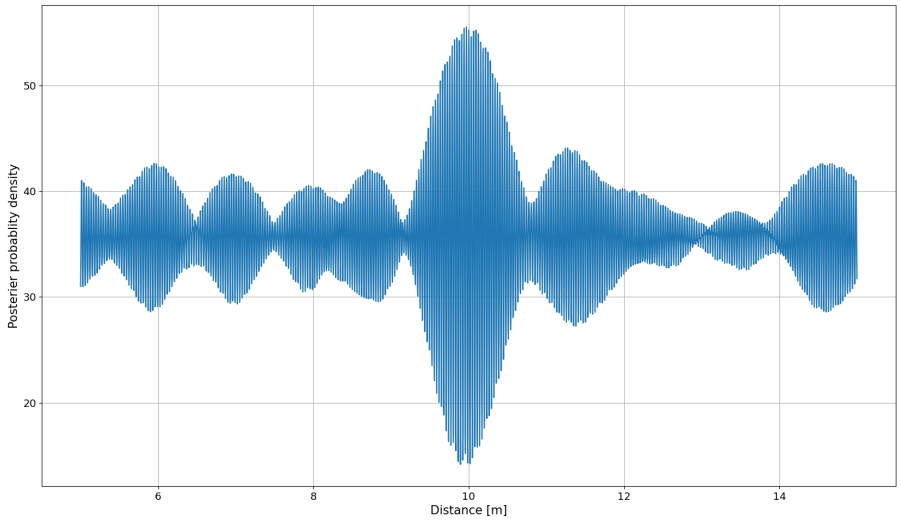

Figure 3.4: Posterior PDF for simulated data for 10 meters at an SNR of 0 dB.

3.2 Distance estimates with different noise

We have performed tests at various SNR to characterize the performance of the estimator at different noise levels. Signals with SNR of 3 dB, 6 dB, 9dB, and 12 dB have been used. For each SNR, 1000 samples are taken. The estimator grid is set up to check every 1.0 mm, while the true distance is also here set to 10.0 meters.

Figure 3.5 shows the results from the simulations with the signal with the highest noise, an SNR of 3 decibels. The histogram shows that around 33% of the samples were calculated to be 10.0 meters. The other distances that were calculated are $\frac{n}{2}\cdot$wavelengths away from the true distance, where $n = \{-3, 3\}$. The other peaks of the sine-wave come from the phase changes for each frequency, which can be seen in equation (2.44), but the noise will cause a spread in the estimator's choice of distance. Table 3.1 summarizes the results. From this, it is shown that the mean range for the signal with an SNR of 3 dB will be 2.3 mm away from the true distance, with a standard deviation of 6.1 cm.

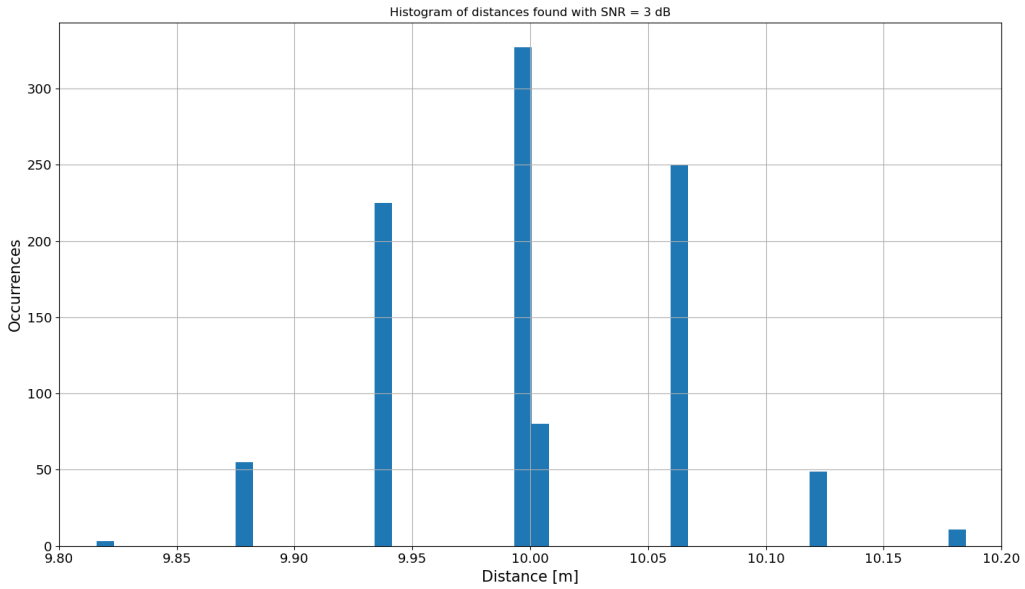

Figure 3.5: Histogram of measured distance with a signal with SNR of 3 dB.

Figure 3.6 shows that when you increase the SNR, the accuracy of the signal is improved. With the results from table 3.1, it is shown that the mean range measured is 0.85 mm away from the real distance. The standard deviation is almost halved, and the mean of the estimated distance is 2.8 cm closer to the correct distance than for the measurements with an SNR of 3 dB.

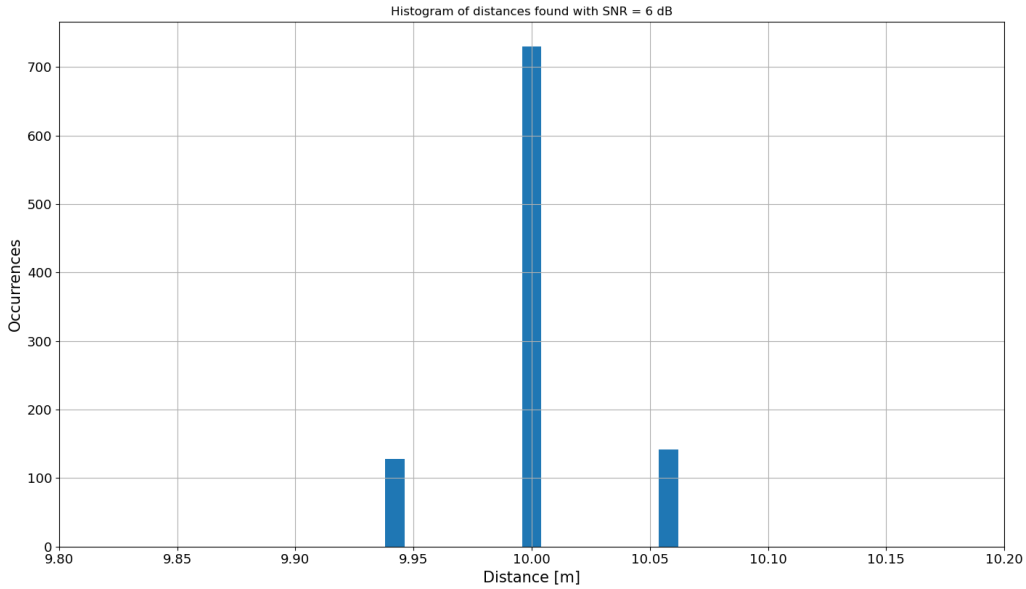

Figure 3.6: Histogram of measured distance with a signal with SNR of 6 dB.

Figure 3.7 shows that with an SNR of 9 dB, the accuracy of the estimate will be even better. The average distance of the estimated distances is 0.18 mm from the actual distance, with a standard deviation of 6.7 mm. In total, 13 samples were not calculated correctly within a millimeter accuracy.

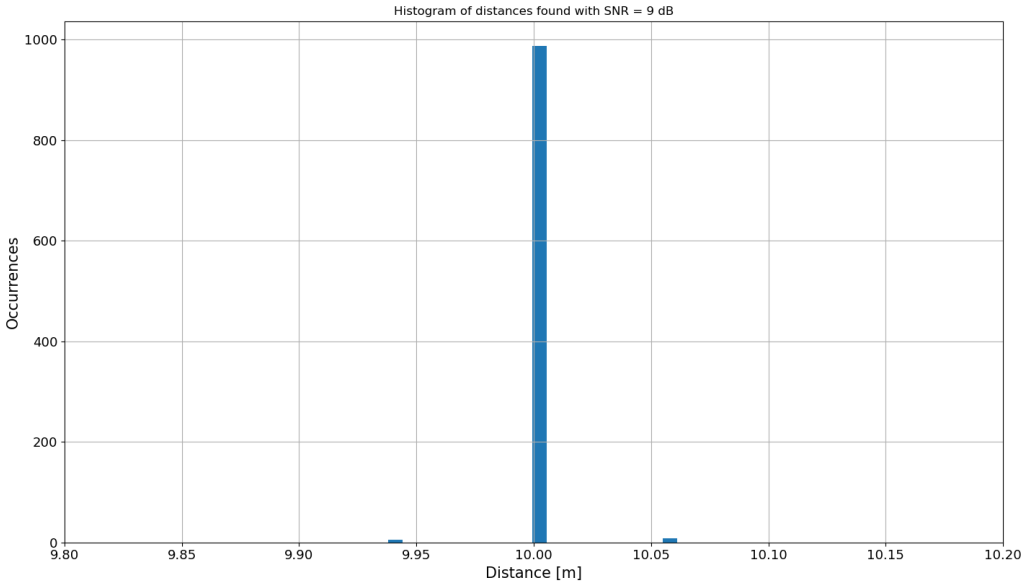

Figure 3.7: Histogram of measured distance with a signal with SNR of 9 dB.

When simulating 1000 measurements with an SNR of 12 dB, the histogram of the estimated distances using equation (2.44) shows that all the measurements came out to be 10.0 meters. Table 3.1 will also show the results for these measurements. Here 1000 of 1000 samples have been estimated correctly within millimeter accuracy, giving a deviation of zero.

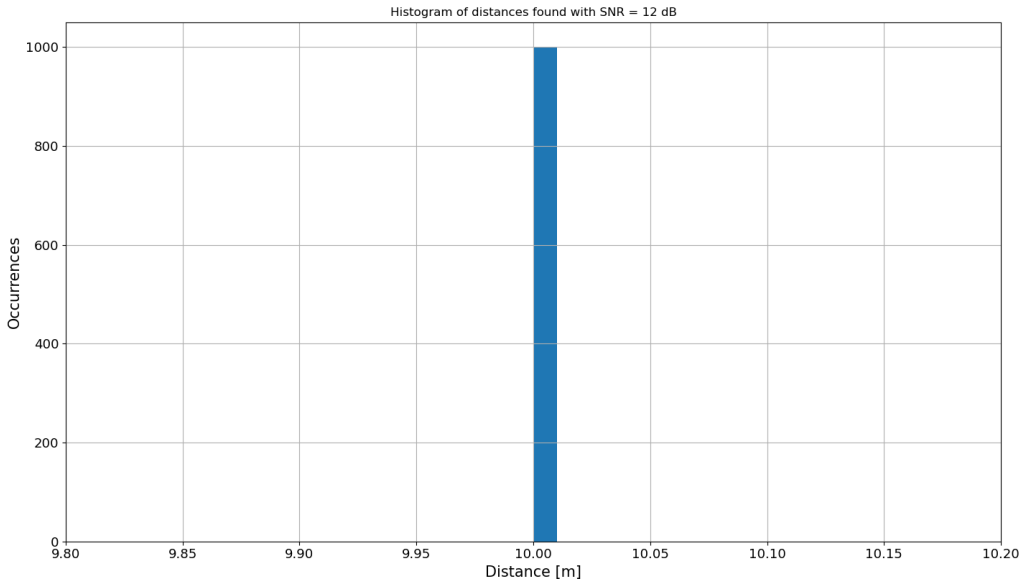

Figure 3.8: Histogram of measured distance with a signal with SNR of 12 dB.

The results from the different signal-to-noise ratios are collected in table 3.1. It shows that the accuracy of the measurements gets better with increasing SNR.

SNR_{dB}	Mean range $\hat{r}_{\text{mean}}[m]$	Standard deviation σ[m]	Variance σ^2[m]	Mean error[m]
3	10.002 284	0.061 835	0.003 824	0.044 642
6	10.000 854	0.031 883	0.001 017	0.016 602
9	10.000 182	0.006 962	0.000 048	0.000 794
12	10.000 000	0.000 000	0.000 000	0.000 000

Table 3.1: Accuracy measurements for different SNRs.

3.3 Estimation errors over distances

To see how the system works for other distances, we will look at the range error as a function of distance. The SNR is set to 7 dB, while we will calculate the error of range estimates from 0 to 100 meters. Figure 3.9 shows the results of the measurement. The distance is estimated every 2.5 cm, with a precision of 1.0 cm in the calculations. The average error is calculated to be 7.2 cm, while the maximum range error is 18.4 cm. This corresponds to three times the wavelength as found earlier in the results.

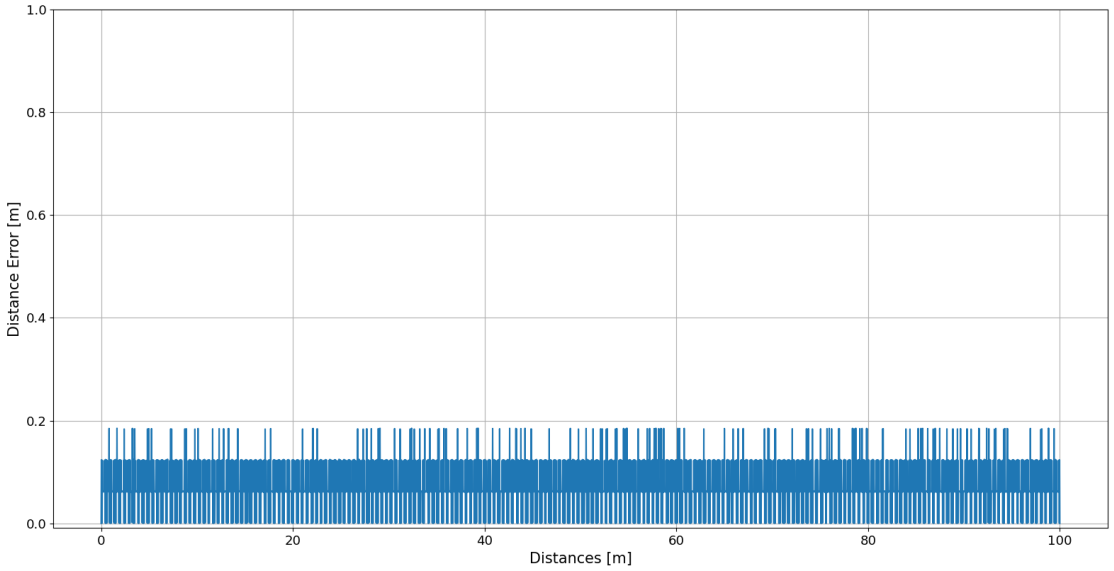

Figure 3.9: Distance error as a function of range.

The figure above shows that the distance error from the estimator will be the same for at all distances, when the noise for them is the same. In a real-world situation, a signal that travels longer will be attenuated more, resulting in lower estimate. This can cause the distance error to increase with the range. This is however not because of the estimator model.

Chapter 4

Discussion

In this section, it will be discussed how the derived range estimate is working, the limitation of the estimate, and what this estimate can be used for.

The focus of this thesis has been to derive a range estimation model for phase measurement over several frequencies. As shown earlier, other papers like [5] and [6] have found an estimate of the two-directional range estimate. The other methods sum the phases together early, removing the phase offset in the devices at the beginning of the derivation. The phase offset will be a nuisance parameter in the measurements. In this derived estimate, we will use the two-directional phase measurements in a different approach. For as long as possible, the two signals will be treated as two separate measurements. We will find the posterior PDF for each of the signals, before trying to combine them. In this way, the characteristics of each measurement are not changed before acknowledging the prior information of them.

One other important difference in using this novel approach for range estimation is that this estimator uses the SNR for each frequency channel when trying to estimate a range. With a changing signal strength for different frequencies, this means that we can smooth the signal strength over the frequency channels, making the measurements found at each frequency count equally.

We have only tested the method on simulated signals with random noise on all frequency channels. As shown in the results, the estimated distances for the simulated data are very accurate. Even at high noise levels with an SNR of 0 dB, the estimator provides a calculation close to the true value.

For the simulated signal with an SNR of 3 dB, the average estimated range for 1000 samples was 2.2 mm over the true distance. An SNR of 3 dB is for a radio signal not very much, so since the accuracy is so high, it will indicate that we have derived a good estimator.

When setting the SNR to 12 dB, the average estimated distance gives a perfect result. All of the 1000 samples estimated the true distance, giving a standard deviation of 0.0 mm. One reason this could happen, is the numerical resolution in the estimator. In this test, the grid of the estimator was set to check every 1.0 mm. Having a higher resolution could lead to a non-zero standard deviation, if this is wanted. But this will lead to an increased computing time.

4.1 Limitations

For a real signal however, other issues should also be taken into consideration. The propagation path of the signal, will not always be a straight path from one device to the other. There can be something blocking the LoS path, so that the signal must travel a longer distance before reaching the other device. A longer distance to travel means there will be a change in the phases as well. The propagation path of each direction is then not necessarily the same.

As mentioned in the results, when testing with a real signal, long-distance measurements will be more affected by the environment. This means that the estimation probably will have some decreasing accuracy. But by the looks of the results for low SNR, the estimate is still able to calculate a range not so far from the true value.

We have assumed that the amplitudes are the same for the measured signal and the signal model. The signal will contain some noise, and therefore exact equality between them cannot happen. It is the measured phases that ultimately will be most important in the estimator, but if the amplitudes for some reason differ too much, the assumption we made may not work.

4.2 Future Work

The estimator derived in this thesis shows some promising results for simulated signals, even for a low SNR. For future work, the signal should be tested on real data. Real measurements can contain more noise, which can lead to more inaccurate results.

For the calculation of the distance, we use a brute force method. We check every distance in a pre-defined range and observe which has the highest posterior PDF. When implementing this estimator in a real-time system, a method for limiting this range should be found in order to reduce the computation time. For the simulated signal, this was done manually since we knew the true distance.

The estimator derived here is good for finding the distance between two devices. By knowing the distance between multiple devices, the position could be determined as well. As mentioned in the introduction, this can be implemented for applications like indoor navigation and asset tracking.

Chapter 5

Conclusion

In this thesis, a Bayesian range estimator has been derived and tested on simulated data. It finds the range that maximizes the posterior PDF of a two-directional signal over multiple frequency channels. The derived expression will use the SNR at each frequency channel when calculating which range maximizes the PDF.

The results of the simulated data indicate that a good estimator is found. When looking at 1000 simulated signals with an SNR of 12 dB, all range estimates resulted in a perfect match with the actual distance. When the signal experienced a higher noise level, the accuracy estimate of the distance estimate was possible to calculate. For signals with an SNR of 3 dB, the standard deviation of the estimates was 6.2 cm, while the average estimated range was 2.2 mm higher than the true distance. This is still not high, so we can conclude that this is a good estimator for estimating a range.

Bibliography

[1] K. M. Tan and C. L. Law. 'GPS and UWB Integration for indoor positioning'. In: (2007), pp. 1–5.

[2] B. M. Apps. '*Top 10 Applications of Bluetooth Low Energy*'. In: (2019). URL: https://www.blemobileapps.com/blog/top-10-applications-of-bluetooth-low-energy/. (accessed: 08.01.2023).

[3] M. Gast. *802.11 Wireless Networks: The Definitive Guide*. 2nd ed. Vol. 1. Sebastopol, CA: O'Reilly Media, May 2005, p. 284. ISBN: 0596100523.

[4] S. M. Kay. *Fundamentals of Statistical Signal Processing, Vol. 1: Estimation Theory*. Prentice Hall PTR, 1993.

[5] P. Zand et al. 'A high-accuracy phase-based ranging solution with Bluetooth Low Energy (BLE)'. In: *2019 IEEE Wireless Communications and Networking Conference (WCNC)*. 2019, pp. 1–8. DOI: 10.1109/WCNC.2019.8885791.

[6] M. Pelka, C. Bollmeyer and H. Hellbrück. 'Accurate radio distance estimation by phase measurements with multiple frequencies'. In: *2014 International Conference on Indoor Positioning and Indoor Navigation (IPIN)*. 2014, pp. 142–151. DOI: 10.1109/IPIN.2014.7275478.

[7] J. A. Forbord. *Network positioning using Multi-Carrier-Phase-Difference*. Project report in TFE4580. Jan. 2023.

[8] J. N. Suarez Lojan. *Positioning with MCPD*. Project report in TFE4580. Jan. 2023.

[9] B. S. Proprietary. '*Bluetooth Core Specification v5.1*'. In: (2019).

[10] J. G. Sponås. *Things You Should Know About Bluetooth Range*. 2023. URL: https://blog.nordicsemi.com/getconnected/things-you-should-know-about-bluetooth-range. (accessed: 10.07.2023).

[11] M. Abramowitz and I. A. Stegun. 9th printing. New York: Dover Publications, 1972. Chap. Modified Bessel Functions I and K, pp. 374–377.

Appendix

A Derivation of signal models

This section contains a more thorough derivation of the signal models from chapter 2.3.

One-directional signal with noise

The signal y is given by

$$y = A \cdot e^{j\phi_d} + w, \tag{A.1}$$

where A is the amplitude of the given frequency, ϕ_d is the phase of the given frequency, and w is noise for the measured signal. The phase ϕ_d is uniformly distributed between 0 and 2π and has a probability distribution given by $p(\phi_d) = \frac{1}{2\pi}$. The measured signal will have the shape $y' = B \cdot e^{j\theta}$, where B is the measured amplitude and θ is the measured amplitude.

A posterior PDF must be found to find a suitable estimator.

The posterior PDF of the phase is dependent on the signal and can be found by looking at the prior information we have of the measured signal and the characteristics given the phase, which is given by

$$p(\phi_d|y) = \frac{p(y|\phi_d)p(\phi_d)}{\int_0^{2\pi} p(y|\phi_d)p(\phi_d)d\phi_d}. \tag{A.2}$$

The likelihood function tells us how the signal y is distributed when we are given the model of the phase ϕ_d, and it is given by

$$\begin{aligned} p(y|\phi_d) &= \frac{1}{\sqrt{2\pi\sigma^2}} \cdot \exp\left\{\frac{-|y' - A \cdot e^{j\phi_d}|^2}{2\sigma^2}\right\} \\ &= \frac{1}{\sqrt{2\pi\sigma^2}} \cdot \exp\left\{\frac{-|y'|^2 - |A|^2 + 2 \cdot \text{Re}\left\{y' \cdot Ae^{j\phi_d})\right\}}{2\sigma^2}\right\} \\ &= \frac{1}{\sqrt{2\pi\sigma^2}} \cdot \exp\left\{\frac{-|y'|^2 - |A|^2 + 2AB\cos(\phi_d + \theta)}{2\sigma^2}\right\}. \end{aligned} \tag{A.3}$$

Setting this and the prior PDF into the expression for the posterior PDF, we get a probability given by

$$
\begin{aligned}
p(\phi_d|y) &= \frac{p(y|\phi_d)p(\phi_d)}{\int_0^{2\pi} p(y|\phi_d)p(\phi_d)d\phi_d} \\
&= \frac{\frac{1}{\sqrt{2\pi\sigma^2}} \cdot \exp\left\{\frac{-|y'|^2-|A|^2+2AB\cos(\phi_d+\theta)}{2\sigma^2}\right\}\frac{1}{2\pi}}{\int_0^{2\pi} \frac{1}{\sqrt{2\pi\sigma^2}} \cdot \exp\left\{\frac{-|y'|^2-|A|^2+2AB\cos(\phi_d+\theta)}{2\sigma^2}\right\}\frac{1}{2\pi}\, d\phi_d} \\
&= \frac{\exp\left\{\frac{AB\cos(\phi_d+\theta)}{\sigma^2}\right\}}{\int_0^{2\pi} \exp\left\{\frac{AB\cos(\phi_d+\theta)}{\sigma^2}\right\} d\phi_d} \\
&= \frac{\exp\left\{\frac{AB\cos(\phi_d+\theta)}{\sigma^2}\right\}}{2\pi I_0\left(\frac{AB}{\sigma^2}\right)},
\end{aligned}
\tag{A.4}
$$

where $I_0(\cdot)$ represents the modified Bessel function. By using MAP estimation, the phase estimate will be given by

$$
\begin{aligned}
\hat{\phi_d} &= \arg\max_{\phi_d} p(\phi_d|y) \\
&= \arg\max_{\phi_d} \frac{\exp\left\{\frac{AB\cos(\phi_d+\theta)}{\sigma^2}\right\}}{2\pi I_0\left(\frac{AB}{\sigma^2}\right)} \\
&= \arg\max_{\phi_d} \cos(\phi_d+\theta) \\
&= -\theta + n\cdot 2\pi
\end{aligned}
\tag{A.5}
$$

where n is an integer.

One-directional range estimation with noise and phase offset

Now, we are looking at a one-directional with both a phase offset $\Delta\phi$ and noise w. The signal model is now given by

$$
y = A\cdot e^{j(\phi_d+\Delta\phi)} + w. \tag{A.6}
$$

The measured signal will have the form $y' = B\cdot e^{j(-\theta+\Delta\phi)}$. The phase offset is not relevant in our estimations and will be treated as a nuisance parameter that we will try to remove, but is uniformly distributed between 0 and 2π. $\Delta\phi$ has the prior probability of $p(\Delta\phi) = \frac{1}{2\pi}$. For the posterior PDF, this means we have an equation given by

$$
p(\phi_d|y) = \int_0^{2\pi} p(\phi_d, \Delta\phi|y)\, d\Delta\phi \tag{A.7}
$$

Both ϕ_d and $\Delta\phi$ are uniformly distributed between 0 and 2π, which gives the posterior PDF to be given by

$$
p(\phi_d, \Delta\phi|y) = \frac{p(y|\phi_d,\Delta\phi)p(\phi_d,\Delta\phi)}{\int_0^{2\pi}\int_0^{2\pi} p(y|\phi_d,\Delta\phi)p(\phi_d,\Delta\phi)\, d\phi_d\, d\Delta\phi}. \tag{A.8}
$$

The probability function of ϕ_d and $\Delta\phi$ will be independent of each other and given by $p(\phi_d, \Delta\phi) = p(\phi_d)\, p(\Delta\phi) = \frac{1}{4\pi^2}$. The likelihood function for y will then be

$$\begin{aligned}
p(y|\phi_d, \Delta\phi) &= \frac{1}{\sqrt{2\pi\sigma^2}} \cdot \exp\left\{\frac{-|y' - A \cdot e^{j(\phi_d+\Delta\phi)}}{2\sigma^2}\right\} \\
&= \frac{1}{\sqrt{2\pi\sigma^2}} \cdot \exp\left\{\frac{-|y'|^2 - |A|^2 + 2AB \cdot \mathsf{Re}\left\{e^{j(\phi_d+2\Delta\phi+\theta)}\right\}}{2\sigma^2}\right\} \\
&= \frac{1}{\sqrt{2\pi\sigma^2}} \cdot \exp\left\{\frac{-|y'|^2 - |A|^2 + 2AB \cdot \mathsf{Re}\left\{\cos(\phi_d + 2\Delta\phi - \theta) + j\sin(\phi_d + 2\Delta\phi - \theta)\right\}}{2\sigma^2}\right\} \\
&= \frac{1}{\sqrt{2\pi\sigma^2}} \cdot \exp\left\{\frac{-|y'|^2 - |A|^2 + 2AB\cos(\phi_d + 2\Delta\phi - \theta)}{2\sigma^2}\right\}.
\end{aligned} \tag{A.9}$$

The posterior PDF still including the nuisance parameter will then be

$$\begin{aligned}
p(\phi_d, \Delta\phi|y) &= \frac{p(y|\phi_d, \Delta\phi)p(\phi_d, \Delta\phi)}{\int_0^{2\pi}\int_0^{2\pi} p(y|\phi_d, \Delta\phi)p(\phi_d, \Delta\phi)\, d\phi_d\, d\Delta\phi} \\
&= \frac{\frac{1}{\sqrt{2\pi\sigma^2}} \cdot \exp\left\{\frac{-|y'|^2-|A|^2+2AB\cos(\phi_d+2\Delta\phi-\theta)}{2\sigma^2}\right\}\frac{1}{4\pi^2}}{\int_0^{2\pi}\int_0^{2\pi} \frac{1}{\sqrt{2\pi\sigma^2}} \cdot \exp\left\{\frac{-|y'|^2-|A|^2+2AB\cos(\phi_d+2\Delta\phi-\theta)}{2\sigma^2}\right\}\frac{1}{4\pi^2}\, d\phi_d\, d\Delta\phi} \\
&= \frac{\exp\left\{\frac{AB\cos(\phi_d+2\Delta\phi-\theta)}{\sigma^2}\right\}}{\int_0^{2\pi}\int_0^{2\pi} \exp\left\{\frac{AB\cos(\phi_d+2\Delta\phi-\theta)}{\sigma^2}\right\} d\phi_d\, d\Delta\phi} \\
&= \frac{\exp\left\{\frac{AB\cos(\phi_d+2\Delta\phi-\theta)}{\sigma^2}\right\}}{4\pi^2 I_0\left(\frac{AB}{\sigma^2}\right)}.
\end{aligned} \tag{A.10}$$

With values for the amplitude and standard deviation, the denominator of the expression will become a constant. Removing the nuisance parameter $\Delta\phi$ from the expression, the posterior PDF we are left with is given by

$$\begin{aligned}
p(\phi_d|y) &= \int_0^{2\pi} p(\phi_d, \Delta\phi|y)\, d\Delta\phi \\
&= \int_0^{2\pi} \frac{\exp\left\{\frac{AB\cos(\phi_d+2\Delta\phi-\theta)}{\sigma^2}\right\}}{4\pi^2 I_0\left(\frac{AB}{\sigma^2}\right)}\, d\Delta\phi \\
&= \frac{2\pi I_0\left(\frac{AB}{\sigma^2}\right)}{4\pi^2 I_0\left(\frac{AB}{\sigma^2}\right)} \\
&= \frac{1}{2\pi}.
\end{aligned} \tag{A.11}$$

Two-directional signal with noise and phase offset

From here and out, we will look for the range r instead of an estimate of the phase ϕ_d. As mentioned earlier, they are connected with the relationship shown in equation (2.6). From this, it is possible to find that the probability for the range r also is uniformly distributed and given by $p(r) = \frac{2f}{c_0}$. We are also starting to have an estimate of the signal that could look like for multiple

frequencies as well. Therefore the signal in this section is written for a specific frequency f. In this part, we are still looking at a two-direction frequency signal, and have now added noise and phase offset to the model. Our signal is now given by

$$y_1[f] = A_1[f] \cdot e^{j(-\frac{2\pi f r}{c_0} + \Delta\phi[f])} + w_1[f]. \tag{A.12}$$

and

$$y_2[f] = A_2[f] \cdot e^{j(-\frac{2\pi f r}{c_0} - \Delta\phi[f])} + w_2[f]. \tag{A.13}$$

The two signals are independent of each other, which gives the joint PDF to be seen as

$$p(y_1[f], y_2[f]|r, \Delta\phi[f]) = p(y_1[f]|r, \Delta\phi[f]) \cdot p(y_2[f]|r, \Delta\phi[f]). \tag{A.14}$$

The PDF of the signals y_1 and y_2 are similar, but not equal. Here y_1 represents the signal from the initiator to the reflector, while y_2 represents the signal from the reflector to the initiator. The PDF of signal y_1 is given by

$$\begin{aligned}
&p(y_1[f]|r, \Delta\phi[f]) = \frac{1}{\sqrt{2\pi\sigma^2}} \cdot \exp\left\{\frac{-|y_1'[f] - A_1[f] \cdot e^{j(-\frac{2\pi f r}{c_0} + \Delta\phi[f])}|^2}{2\sigma^2}\right\} \\
=&\frac{1}{\sqrt{2\pi\sigma^2}} \cdot \exp\left\{\frac{-|y_1'[f]|^2 - |A_1[f]|^2 + 2A_1[f]B_1[f] \cdot \text{Re}\left\{e^{j(-\frac{2\pi f r}{c_0} + \Delta\phi[f] - \theta_1[f])}\right\}}{2\sigma^2}\right\} \\
=&\frac{1}{\sqrt{2\pi\sigma^2}} \cdot \exp\left\{\frac{\text{-}|y_1'[f]|^2 - |A_1[f]|^2 \text{+} 2A_1[f]B_1[f] \cdot \text{Re}\left\{\cos(\frac{\text{-}2\pi f r}{c_0} \text{+} \Delta\phi[f] - \theta_1[f]) \text{+} j\sin(\frac{\text{-}2\pi f r}{c_0} \text{+} \Delta\phi[f] - \theta_1[f])\right\}}{2\sigma^2}\right\} \\
=&\frac{1}{\sqrt{2\pi\sigma^2}} \exp\left\{\frac{-|y_1'[f]|^2 - |A_1[f]|^2 + 2A_1[f]B_1[f]\cos(-\frac{2\pi f r}{c_0} + \Delta\phi[f] - \theta_1[f])}{2\sigma^2}\right\},
\end{aligned} \tag{A.15}$$

where $y_1'[f] = B_1[f] \cdot e^{-j\theta_1[f]}$ is the observed signal model.

For the signal y_2, the PDF is given by

$$\begin{aligned}
&p(y_2[f]|r, \Delta\phi[f]) = \frac{1}{\sqrt{2\pi\sigma^2}} \cdot \exp\left\{\frac{-|y_2'[f] - A_2[f] \cdot e^{j(-\frac{2\pi f r}{c_0} - \Delta\phi[f])}|^2}{2\sigma^2}\right\} \\
=&\frac{1}{\sqrt{2\pi\sigma^2}} \cdot \exp\left\{\frac{-|y_2'[f]|^2 - |A_2[f]|^2 + 2A_2[f]B_2[f] \cdot \text{Re}\left\{e^{j(-\frac{2\pi f r}{c_0} - \Delta\phi[f] - \theta_2[f])}\right\}}{2\sigma^2}\right\} \\
=&\frac{1}{\sqrt{2\pi\sigma^2}} \cdot \exp\left\{\frac{\text{-}|y_2'[f]|^2 - |A_2[f]|^2 \text{+} 2A_2[f]B_2[f] \cdot \text{Re}\left\{\cos(\frac{\text{-}2\pi f r}{c_0} - \Delta\phi[f] - \theta_2[f]) \text{+} j\sin(\frac{\text{-}2\pi f r}{c_0} - \Delta\phi[f] - \theta_2[f])\right\}}{2\sigma^2}\right\} \\
=&\frac{1}{\sqrt{2\pi\sigma^2}} \exp\left\{\frac{-|y_2[f]|^2 - |A_2[f]|^2 + 2A_2[f]B_2[f]\cos(\frac{\text{-}2\pi f r}{c_0} - \Delta\phi[f] - \theta_2[f])}{2\sigma^2}\right\},
\end{aligned} \tag{A.16}$$

where $y_2'[f] = B_2[f] \cdot e^{-j\theta_2[f]}$ is the observed signal model.

The joint PDF will then become

$$
\begin{aligned}
&p(y_1[f], y_2[f]|r, \Delta\phi[f]) = p(y_1[f]|r, \Delta\phi[f]) \cdot p(y_2[f]|r, \Delta\phi[f]) \\
&= \frac{1}{\sqrt{2\pi\sigma^2}} \exp\left\{ \frac{-|y_1'[f]|^2 - |A_1[f]|^2 + 2A_1[f]B_2[f]\cos(-\frac{2\pi fr}{c_0} + \Delta\phi[f] - \theta_1[f])}{2\sigma^2} \right\} \\
&\cdot \frac{1}{\sqrt{2\pi\sigma^2}} \exp\left\{ \frac{-|y_2[f]|^2 - |A_2[f]|^2 + 2A_2[f]B_2[f]\cos(\frac{-2\pi fr}{c_0} - \Delta\phi[f] - \theta_2[f])}{2\sigma^2} \right\} \\
&= \frac{1}{2\pi\sigma^2} \exp\left\{ \frac{-|y_1[f]|^2 - |y_2[f]|^2 - |A_1[f]|^2 - |A_2[f]|^2}{2\sigma^2} \right\} \\
&\cdot \exp\left\{ \frac{2A_1[f]B_2[f]\cos(-\frac{2\pi fr}{c_0} + \Delta\phi - \theta_1[f]) + 2A_2[f]B_2[f]\cos(-\frac{2\pi fr}{c_0} - \Delta\phi[f] - \theta_2[f])}{\sigma^2} \right\}
\end{aligned}
\tag{A.17}
$$

We are focusing on the phases, and not the amplitudes. We are assuming we know the amplitudes perfectly, such that $A_1 = B_1$ and $A_2 = B_2$. The signal is also assumed to be equally significant when being measured at the reflector, as when it is being measured at the initiator. Due to their nearly identical travel distances and durations, we denote $A_1 = A_2 = A$ henceforth. It is worth emphasizing that the measurements will not yield perfect equality due to inherent measurement noise. However, this assumption simplifies the derivation process, as the precise estimation of amplitudes is not the primary objective.

The joint PDF will therefore be given by

$$
\begin{aligned}
&p(y_1[f], y_2[f]|r, \Delta\phi[f]) \\
&= \frac{1}{2\pi\sigma^2} \exp\left\{ \frac{-|y_1[f]|^2 - |y_2[f]|^2 - 2|A[f]|^2}{2\sigma^2} \right\} \\
&\cdot \exp\left\{ \frac{2A[f]^2\cos(-\frac{2\pi fr}{c_0} + \Delta\phi - \theta_1[f]) + 2A[f]^2\cos(-\frac{2\pi fr}{c_0} - \Delta\phi[f] - \theta_2[f])}{\sigma^2} \right\} \\
&= \frac{1}{2\pi\sigma^2} \exp\left\{ \frac{-|y_1'[f]|^2 - |y_2'[f]|^2 - 2|A[f]|^2}{2\sigma^2} \right\} \\
&\cdot \exp\left\{ \frac{A[f]^2\left(\cos(-\frac{2\pi fr}{c_0} - \theta_1[f]) + \cos(-\frac{2\pi fr}{c_0} - \Delta\phi[f] - \theta_2[f])\right)}{\sigma^2} \right\} \\
&= \frac{1}{2\pi\sigma^2} \exp\left\{ \frac{-|y_1'[f]|^2 - |y_2'[f]|^2 - 2|A[f]|^2}{2\sigma^2} \right\} \\
&\cdot \exp\left\{ \frac{2A[f]^2\left(\cos(\frac{-\frac{2\pi fr}{c_0} - \theta_1[f] + (-\frac{2\pi fr}{c_0} - \Delta\phi[f] - \theta_2[f])}{2})\cos(\frac{-\frac{2\pi fr}{c_0} - \theta_1[f] - (-\frac{2\pi fr}{c_0} - \Delta\phi[f] - \theta_2[f])}{2})\right)}{\sigma^2} \right\} \\
&= \frac{1}{2\pi\sigma^2} \exp\left\{ \frac{-|y_1'[f]|^2 - |y_2'[f]|^2 - 2|A[f]|^2}{2\sigma^2} \right\} \\
&\cdot \exp\left\{ \frac{2A[f]^2\left(\cos(\frac{2\pi fr}{c_0} + \frac{\theta_1[f] + \theta_2[f]}{2})\cos(\Delta\phi[f] - \frac{\theta_1[f] - \theta_2[f]}{2})\right)}{\sigma^2} \right\},
\end{aligned}
\tag{A.18}
$$

where we use the trigonometric identity $\cos(a) + \cos(b) = 2\cos(\frac{a+b}{2})\cos(\frac{a-b}{2})$ and $\cos(x) = \cos(-x)$.

The probability of both r and $\Delta\phi$ is constant and independent, which gives the probability of both of them to be $p(r, \Delta\phi) = \frac{f}{\pi c_0}$. By adding these to the posterior distribution for r and $\Delta\phi$, we get that the probability is dependent on

$$p(r, \Delta\phi[f]|y_1[f], y_2[f]) = \frac{p(y_1[f], y_2[f]|r, \Delta\phi[f])p(r, \Delta\phi[f])}{\int_0^{2\pi}\int_0^{\frac{-c_0}{f}} p(y_1[f], y_2[f]|r, \Delta\phi[f])p(r, \Delta\phi[f])\, dr\, d\Delta\phi} \tag{A.19}$$

$$= \frac{\frac{1}{2\pi\sigma^2}\exp\left\{\frac{-|y_1'[f]|^2-|y_2'[f]|^2-2|A[f]|^2}{2\sigma^2}+\frac{2A[f]^2\left(\cos(\frac{2\pi fr}{c_0}+\frac{\theta_1[f]+\theta_2[f]}{2})\cos(\Delta\phi[f]-\frac{\theta_1[f]-\theta_2[f]}{2})\right)}{\sigma^2}\right\}\frac{f}{\pi c_0}}{\int_0^{2\pi}\int_0^{\frac{-c_0}{f}} \frac{1}{2\pi\sigma^2}\exp\left\{\frac{-|y_1'[f]|^2-|y_2'[f]|^2-2|A[f]|^2}{2\sigma^2}+\frac{2A[f]^2\cos(\frac{2\pi fr}{c_0}+\frac{\theta_1[f]+\theta_2[f]}{2})\cos(\Delta\phi[f]-\frac{\theta_1[f]-\theta_2[f]}{2})}{\sigma^2}\right\}\frac{f}{\pi c_0}\, dr\, d\Delta\phi} \tag{A.20}$$

$$= \frac{\exp\left\{\frac{2A[f]B[f](\cos(-\frac{2\pi fr}{c_0}+\frac{\theta_1[f]+\theta_2[f]}{2})\cos(\Delta\phi[f]+\frac{\theta_1[f]-\theta_2[f]}{2}))}{\sigma^2}\right\}}{\int_0^{2\pi}\int_0^{-\frac{c_0}{f}} \exp\left\{\frac{2A[f]B[f](\cos(-\frac{2\pi fr}{c_0}+\frac{\theta_1[f]+\theta_2[f]}{2})\cos(\Delta\phi[f]+\frac{\theta_1[f]-\theta_2[f]}{2}))}{\sigma^2}\right\} dr\, d\Delta\phi} \tag{A.21}$$

$$= \frac{\exp\left\{\frac{2A[f]^2(\cos(-\frac{2\pi fr}{c_0}+\frac{\theta_1[f]+\theta_2[f]}{2})\cos(\Delta\phi[f]+\frac{\theta_1[f]-\theta_2[f]}{2}))}{\sigma^2}\right\}}{K_n[f]}. \tag{A.22}$$

Since the expression $\frac{1}{2\pi\sigma^2}\exp\left\{\frac{-|y_1'[f]|^2-|y_2'[f]|^2-2|A[f]|^2}{2\sigma^2}\right\}$ is not dependent on r or $\Delta\phi$, it can be moved out of the integral in the denominator. Then it can be crossed out with the expression in the nominator. K_n is then the remaining part of the denominator, and will be a normalizing factor that does not affect the extreme points when trying to find the distance r. K_n is given by

$$K_n = \int_0^{2\pi}\int_0^{-\frac{c_0}{f}} \cdot \exp\left\{\frac{2A[f]^2\left(\cos(\frac{2\pi fr}{c_0}+\frac{\theta_1[f]+\theta_2[f]}{2})\cos(\Delta\phi[f]-\frac{\theta_1[f]-\theta_2[f]}{2})\right)}{\sigma^2}\right\} dr\, d\Delta\phi. \tag{A.23}$$

The next step is to remove the phase offset $\Delta\phi$, because this is a nuisance parameter. The nuisance parameter can be integrated away, giving us an expression for the posterior PDF of the range:

$$\begin{aligned} p(r|y_1[f], y_2[f]) &= \int_0^{2\pi} p(r, \Delta\phi|y_1[f], y_2[f])\, d\Delta\phi \\ &= \int_0^{2\pi} \frac{\exp\left\{\frac{2A[f]^2(\cos(\frac{2\pi fr}{c_0}+\frac{\theta_1[f]+\theta_2[f]}{2})\cos(\Delta\phi[f]+\frac{\theta_1[f]-\theta_2[f]}{2}))}{\sigma^2}\right\}}{K_n[f]} d\Delta\phi \\ &= \frac{2\pi}{K_n[f]} \cdot I_0\left(\frac{2A[f]^2}{\sigma^2}\cdot\cos\left(\frac{2\pi fr}{c_0}+\frac{\theta_1[f]+\theta_2[f]}{2}\right)\right). \end{aligned} \tag{A.24}$$

To find an estimate of r, the maximum a posteriori (MAP) probability estimation can be used. This

involves finding the argument r that maximizes the posterior probability that we found above:

$$\begin{aligned}\hat{r}[f] &= \arg\max_r \; p(r|y_1[f], y_2[f]) \\ &= \arg\max_r \; \frac{2\pi}{K_n} \cdot I_0\left(\frac{2A[f]B[f]}{\sigma^2} \cdot \cos\left(-\frac{2\pi f r}{c_0} + \frac{\theta_1[f] + \theta_2[f]}{2}\right)\right).\end{aligned} \tag{A.25}$$

The equation above is maximized when the inside of the brackets to the cosine equals zero. This gives us that the MAP estimate of r is given by

$$\hat{r}[f] = \frac{c_0}{4\pi}\frac{\theta_1[f] + \theta_2[f]}{f}, \tag{A.26}$$

where θ_1 and θ_2 represent the angle of arrival of the signal at the initiator and reflector, respectively.

With multiple frequencies

This is the part for multiple frequencies.

The joint probability for two frequencies in the signal model described over will be given by

$$\begin{aligned}p(r|y_1[f_1], y_2[f_1], y_1[f_2], y_2[f_2]) &= \int_0^{2\pi}\int_0^{2\pi} p(r, \Delta\phi_1, \Delta\phi_2|y_1[f_1], y_2[f_1], y_1[f_2], y_2[f_2])\, d\Delta\phi_1\, d\Delta\phi_2 \\ &= \int_0^{2\pi}\int_0^{2\pi} p(r, \Delta\phi_1, \Delta\phi_2|y_1[f_1], y_2[f_1]) \cdot p(r, \Delta\phi_1, \Delta\phi_2|y_1[f_2], y_2[f_2])\, d\Delta\phi_1\, d\Delta\phi_2 \\ &= \int_0^{2\pi}\int_0^{2\pi} p(r, \Delta\phi_1|y_1[f_1], y_2[f_1]) \cdot p(r, \Delta\phi_2|y_1[f_2], y_2[f_2])\, d\Delta\phi_1\, d\Delta\phi_2 \\ &= \int_0^{2\pi} p(r, \Delta\phi_1|y_1[f_1], y_2[f_1])\, d\Delta\phi_1 \cdot \int_0^{2\pi} p(r, \Delta\phi_2|y_1[f_2], y_2[f_2])\, d\Delta\phi_2 \\ &= p(r|y_1[f_1], y_2[f_1]) \cdot p(r|y_1[f_2], y_2[f_2]).\end{aligned} \tag{A.27}$$

The second equation comes from the fact that the two measurements for different frequencies are independent of each other. The third equation above can be shown to be correct, because $y_1[f_1]$ and $y_2[f_1]$ are not dependent on $\Delta\phi_2$, while $y_1[f_2]$ and $y_2[f_2]$ are not dependent on $\Delta\phi_1$.

Here it is possible to insert the equation found in (2.37), for each of the frequencies. The equation for the posterior is now given by

$$\begin{aligned}&p(r|y_1[f_1], y_2[f_1], y_1[f_2], y_2[f_2]) \\ &\quad = p(r|y_1[f_1], y_2[f_1]) \cdot p(r|y_1[f_2], y_2[f_2]) \\ &= \frac{2\pi}{K_{n1}} \cdot I_0\left(\frac{2A[f_1]^{"}}{\sigma^2} \cdot \cos\left(\frac{2\pi f_1 r}{c_0} + \frac{\theta_1[f_1] + \theta_2[f_1]}{2}\right)\right) \\ &\quad \cdot \frac{2\pi}{K_{n2}} \cdot I_0\left(\frac{2A[f_2]^2}{\sigma^2} \cdot \cos\left(\frac{2\pi f_2 r}{c_0} + \frac{\theta_1[f_2] + \theta_2[f_2]}{2}\right)\right).\end{aligned} \tag{A.28}$$

MAP can also here be used to find the estimate of the distance. MAP for this function is found by:

$$\begin{aligned}
\hat{r} &= \arg\max_r \; p(r|y_1[f_1], y_2[f_1], y_1[f_2], y_2[f_2]) \\
&= \arg\max_r \; \frac{2\pi}{K_n[f_1]} \cdot I_0\left(2\frac{A[f_1]^2}{\sigma^2} \cdot \cos\left(\frac{2\pi f_1 r}{c_0} + \frac{\theta_1[f_1] + \theta_2[f_1]}{2}\right)\right) \\
&\quad \cdot \frac{2\pi}{K_n[f_2]} \cdot I_0\left(2\frac{A[f_2]^2}{\sigma^2} \cdot \cos\left(\frac{2\pi f_2 r}{c_0} + \frac{\theta_1[f_2] + \theta_2[f_2]}{2}\right)\right) \\
&= \arg\max_r \; \left(\log\left(I_0\left(\frac{2A[f_1]^2}{\sigma^2} \cdot \cos\left(\frac{2\pi f_1 r}{c_0} + \frac{\theta_1[f_1] + \theta_2[f_1]}{2}\right)\right)\right)\right. \\
&\quad \left. + \log\left(I_0\left(\frac{2A[f_2]^2}{\sigma^2} \cdot \cos\left(\frac{2\pi f_2 r}{c_0} + \frac{\theta_1[f_2] + \theta_2[f_2]}{2}\right)\right)\right)\right).
\end{aligned} \tag{A.29}$$

This can be rewritten to be a sum of the two frequencies

$$\hat{r} = \arg\max_r \sum_{i=1}^{2} \log\left(I_0\left(\frac{2A[f_i]^2}{\sigma^2} \cdot \cos\left(\frac{2\pi f_i r}{c_0} + \frac{\theta_1[f_i] + \theta_2[f_i]}{2}\right)\right)\right). \tag{A.30}$$

And now this can be expanded for multiple frequencies. This

$$\hat{r} = \arg\max_r \sum_{i=1}^{K_f} \log\left(I_0\left(\frac{2A[f_i]^2}{\sigma^2} \cdot \cos\left(\frac{2\pi f_i r}{c_0} + \frac{\theta_1[f_i] + \theta_2[f_i]}{2}\right)\right)\right). \tag{A.31}$$

B Review of the MMSE derivation

This part will review the expression by using the MMSE estimator, and some thoughts about why a solution was not found.

The MMSE equation is given by

$$\tilde{r} = \int_0^{\frac{c_0}{f}} r \cdot \frac{2\pi}{K_n[f]} \cdot I_0\left(\frac{2A[f]^2}{\sigma^2} \cdot \cos\left(\frac{2\pi f r}{c_0} + \frac{\theta_1[f] + \theta_2[f]}{2}\right)\right) dr, \tag{B.1}$$

where K_n is given by

$$K_n = \int_0^{2\pi} \int_0^{-\frac{c_0}{f}} \exp\left\{\frac{2A[f]^2\left(\cos(\frac{2\pi f r}{c_0} + \frac{\theta_1[f]+\theta_2[f]}{2})\cos(\Delta\phi[f] - \frac{\theta_1[f]-\theta_2[f]}{2})\right)}{\sigma^2}\right\} dr\, d\Delta\phi. \tag{B.2}$$

K_n will be a normalizing constant, not dependent on r, we move that outside the integral.

We will first try to solve the variable change to make the expression easier. We set $u = \frac{2\pi f r}{c_0} + \frac{\theta_1[f]+\theta_2[f]}{2}$, giving us $r = (u - \frac{\theta_1[f]+\theta_2[f]}{2}) \cdot \frac{c_0}{2\pi f}$. The limits of the integral will now be: $[\frac{\theta_1[f]+\theta_2[f]}{2}, 2\pi + \frac{\theta_1[f]+\theta_2[f]}{2}] = [0, 2\pi]$. Putting that into equation (B.1), we get

$$\tilde{r} = \frac{c_0}{f \cdot K_n[f]} \cdot \int_0^{2\pi} (u - \frac{\theta_1[f] + \theta_2[f]}{2}) \cdot I_0\left(\frac{2A[f]^2}{\sigma^2} \cdot \cos(u)\right) du \tag{B.3}$$

When trying to integrate the first part of (B.3), we have u in two places inside the integral. We try integration by parts.

With a starting point in (C.4), we set w and v to be

$$\begin{aligned} w' &= u - (\frac{\theta_1[f] + \theta_2[f]}{2}) \\ w &= \frac{1}{2}u^2 - (\frac{\theta_1[f] + \theta_2[f]}{2}) \cdot u \\ v &= I_0\left(\frac{2A[f]^2}{\sigma^2} \cdot \cos(u)\right) \\ v' &= \exp\left\{\frac{2A[f]^2}{\sigma^2} \cdot \cos(u) \cdot cos(c \cdot u)\right\}, \end{aligned}$$

where c is a constant.

Setting these values in, we get

$$\begin{aligned} \tilde{r} &= \frac{2\pi}{K_n[f]} \cdot \int_0^{2\pi} (u - \frac{\theta_1[f] + \theta_2[f]}{2}) \cdot I_0\left(\frac{2A[f]^2}{\sigma^2} \cdot \cos(u)\right) du \cdot \frac{c_0}{2\pi f} \\ &= \frac{c_0}{f \cdot K_n[f]} \left[(\frac{1}{2}u^2 - (\frac{\theta_1[f] + \theta_2[f]}{2}) \cdot u) \cdot I_0\left(\frac{2A[f]^2}{\sigma^2} \cdot \cos(u)\right)\right] \\ &- \frac{c_0}{f \cdot K_n[f]} \int_0^{2\pi} (\frac{1}{2}u^2 - (\frac{\theta_1[f] + \theta_2[f]}{2}) \cdot u) \exp\left\{\frac{2A[f]^2}{\sigma^2} \cdot \cos(u) \cdot cos(c \cdot u)\right\} du. \end{aligned} \tag{B.4}$$

which gives an expression that again has multiple variables with u.

If we try to change the variables

$$
\begin{aligned}
w &= u - (\frac{\theta_1[f] + \theta_2[f]}{2}) \\
w' &= 1 \\
v' &= I_0\left(\frac{2A[f]^2}{\sigma^2} \cdot \cos(u)\right) \\
v &= \int_0^{2\pi} I_0\left(\frac{2A[f]^2}{\sigma^2} \cdot \cos(u)\right) du,
\end{aligned}
$$

We now have to solve the integral of the modified Bessel function, where the argument is the same as we are integrating over.

$$
\begin{aligned}
\tilde{r} &= \frac{2\pi}{K_n[f]} \cdot \int_0^{2\pi} (u - \frac{\theta_1[f] + \theta_2[f]}{2}) \cdot I_0\left(\frac{2A[f]^2}{\sigma^2} \cdot \cos(u)\right) du \cdot \frac{c_0}{2\pi f} \\
&= \frac{c_0}{f \cdot K_n[f]} \left[(u - (\frac{\theta_1[f] + \theta_2[f]}{2})) \cdot \int I_0\left(\frac{2A[f]^2}{\sigma^2} \cdot \cos(u)\right) \right]_0^{2\pi} \\
&- \frac{c_0}{f \cdot K_n[f]} \int_0^{2\pi} 1 \cdot \int_0^{2\pi} I_0\left(\frac{2A[f]^2}{\sigma^2} \cdot \cos(u)\right) du\, du.
\end{aligned}
\tag{B.5}
$$

Here it looks like the equation will just go into a loop, and the expression will be even uglier. We will get a non-trivial expression, and chooses therefore not to follow this further.

C Useful functions

This section contains functions that have been very useful in the derivation of the expression.

Modified Bessel function

The modified Bessel function is a function used for solving integrals with functions inside the exponent. The modified Bessel function is found in [11], and given by

$$\frac{1}{\pi}\int_0^{\pi} e^{z\cdot\cos(\theta)}\cos(n\theta)d\theta = I_n(z) = \sum_{m=0}^{\infty}\frac{1}{m!\cdot\Gamma(m+n+1)}\left(\frac{z}{2}\right)^{2m+n}. \tag{C.1}$$

The version of this that is most used in this thesis, is when $n = 0$, which gives the expression:

$$\pi\cdot I_0(z) = \int_0^{\pi} e^{z\cdot\cos(\theta)}\,d\theta \tag{C.2}$$

Signal-to-noise ratio

The Signal-to-Noise Ratio (SNR) in decibel, can be found by taking the logarithmic of the signal amplitude, divided by the variance, or

$$SNR_{dB} = 10\cdot\log_{10}\left(\frac{A^2}{\sigma^2}\right), \tag{C.3}$$

where A is the amplitude, and σ^2 is the variance of the signal.

Integration by parts

The formula for integration by parts is given by

$$\int_a^b u(x)\cdot v'(x)dx = [u(x)\cdot v(x)]_a^b - \int_a^b u'(x)\cdot v(x)dx. \tag{C.4}$$

D Code for simulating a two-directional measurement with multiple frequencies

```
import matplotlib.pyplot as plt
import numpy as np


# First set up the simulated signal.
c0= 299792458 #speed of light
true_range = 10
l_freq = 80          # number of frequency channels

# Simulate simple amplitudes of length given over.
local_amplitude = [1]* l_freq
remote_amplitude = [1]* l_freq

# Var is given in numbers, not decibel.
var= 0.5
# generate random complex noise
n1=np.random.normal(0,var/np.sqrt(2),size=l_freq)+1j*np.random.normal(0,var/np.sqrt(2),size=l_freq)
n2=np.random.normal(0,var/np.sqrt(2),size=l_freq)+1j*np.random.normal(0,var/np.sqrt(2),size=l_freq)


## Frequencies is from the freq-band to BLE
freq= np.linspace(2.4e9,2.4835e9,l_freq)

#first set up angles how they should be
loc_ang_noisefree  = -2*np.pi*freq*true_range/c0
rem_ang_noisefree = -2*np.pi*freq*true_range/c0

# make signal model with noise
y_local  = np.multiply(loc_amp, np.exp(1j*loc_ang_noisefree)) + noise1
y_remote = np.multiply(rem_amp,np.exp(1j*rem_ang_noisefree))+ noise2

# find the angle from signal model
ang_local = np.angle(y_local)
ang_remote = np.angle(y_remote)

# find the amplitudes from signal model
real_local = [ele.real**2 for ele in y_local]
imag_local = [ele.imag**2 for ele in y_local]
amplitude_local = np.sqrt([ real_local[x] + imag_local[x] for x in range(len(imag_local))])

real_remote = [ele.real**2 for ele in y_remote]
imag_remote = [ele.imag**2 for ele in y_remote]
amplitude_remote = np.sqrt([ real_remote[x] + imag_remote[x] for x in range(len(imag_remote))])
```

```
56
57  # Function for finding the distance value that has the highest posterior PDF
58  def loop_distances(local_amp,remote_amp,var,freq,local_ang,remote_ang,c0):
59
60      distances = np.linspace(8,12,4001)       #our search-area, the grid
61      pdf_plot = []
62      last_pdf = False
63      argmax_dist = 0
64      dist_plot = []
65
66      # For distances in search-area, find which is bigger
67      for r in distances:
68          curr_pdf = pdf_equation(r,local_amp,remote_amp,var,freq,local_ang,remote_ang,c0)
69          pdf_plot.append(curr_pdf)
70          dist_plot.append(r)
71          if last_pdf == False:
72              last_pdf = curr_pdf
73              argmax_dist = r
74          elif np.abs(curr_pdf)>= np.abs(last_pdf):
75              last_pdf = curr_pdf
76              argmax_dist = r
77      return argmax_dist, dist_plot,pdf_plot
78
79  # The equation we want to calculate
80  def pdf_equation(x, local_amplitude, remote_amplitude, var, f, local_angle, remote_angle, c0):
81      result = 0
82      n = len(local_amplitude)
83      inside_cos_part =[]
84      phases = []
85      angle_diffs = []
86      #For every frequency sample, a term is added and summed up
87      for i in range(n):
88          phase = -2*np.pi*f[i]*x/c0#+2*np.pi*f[0]*x/c0
89          angle_diff = (local_angle[i]+remote_angle[i])/2
90          phases.append(np.exp(1j*phase))
91          angle_diffs.append(angle_diff)
92      phases = np.unwrap(np.angle(phases))
93      angle_diffs = np.unwrap(angle_diffs)
94      for i in range(n):
95          inside_cos = phases[i]-angle_diffs[i]
96          inside_cos_part.append(inside_cos)
97      inside_cos_part = np.unwrap(inside_cos_part,period = np.pi)
98      for i in range(n):
99          cos_func =np.cos(inside_cos_part[i])
100         amplituder = 2*local_amplitude[i]*remote_amplitude[i]/(var)
101         bessel_func = np.i0(amplituder*cos_func)
102         term = np.log10(bessel_func)
103         result += term
104     return result
105
106 dist,dist_plot,pdf_plot = loop_distances(local_amp,remote_amp,var,freq,ang_local,ang_remote,c0)
107
108 print("FOUND DIST gives = {} meters".format(dist))
109 print("TRUE DIST = {} meters".format(true_range))
110 plt.grid()
111 plt.plot(dist_plot,pdf_plot)
112 plt.xlabel("Distance [m]")
113 plt.ylabel("Posterier probablity density")
114 plt.show()
```

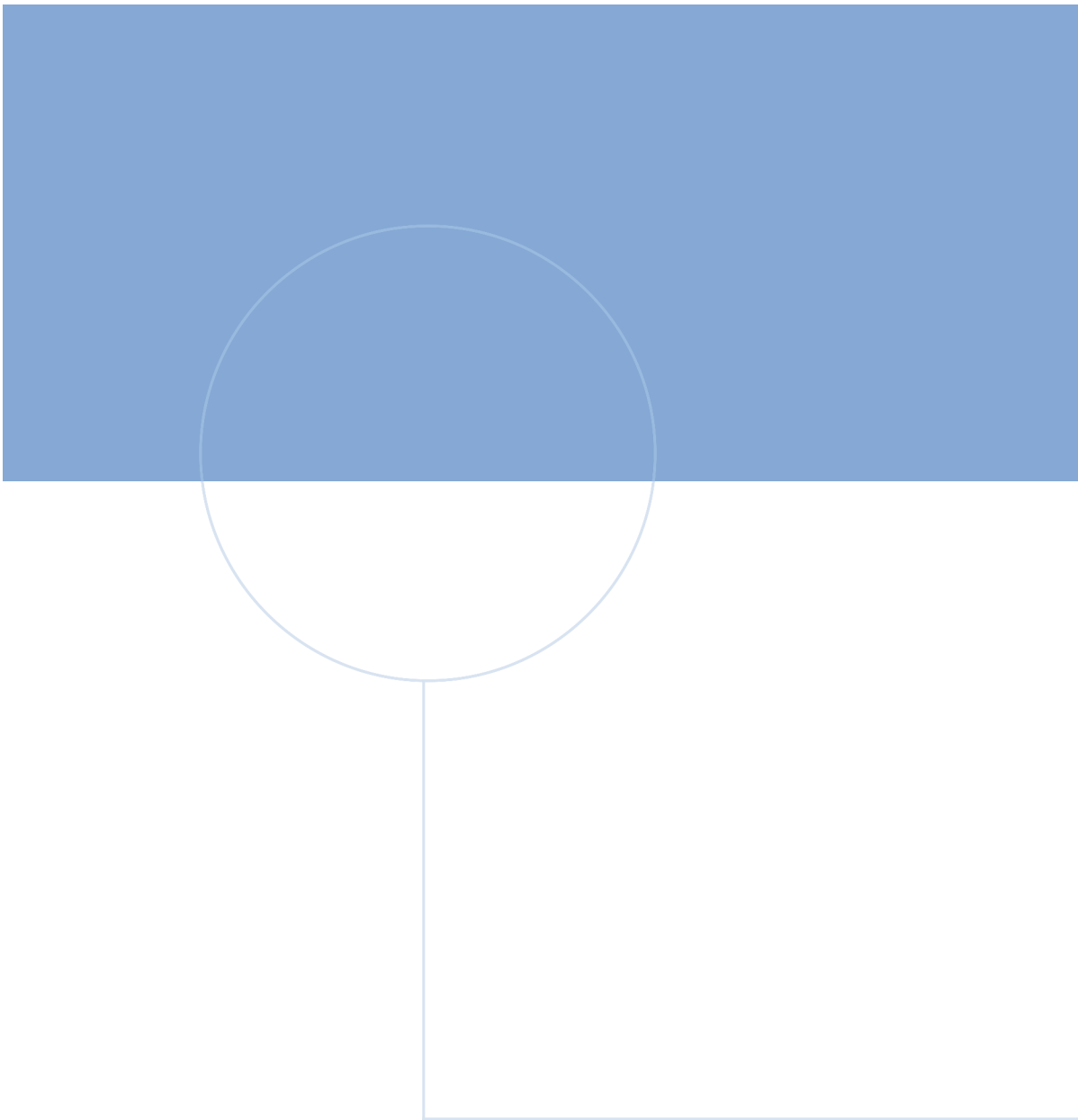

NTNU

Norwegian University of
Science and Technology